Molecular Cell

Article

A pair of readers of bivalent chromatin mediate formation of Polycomb-based "memory of cold" in plants

Graphical abstract

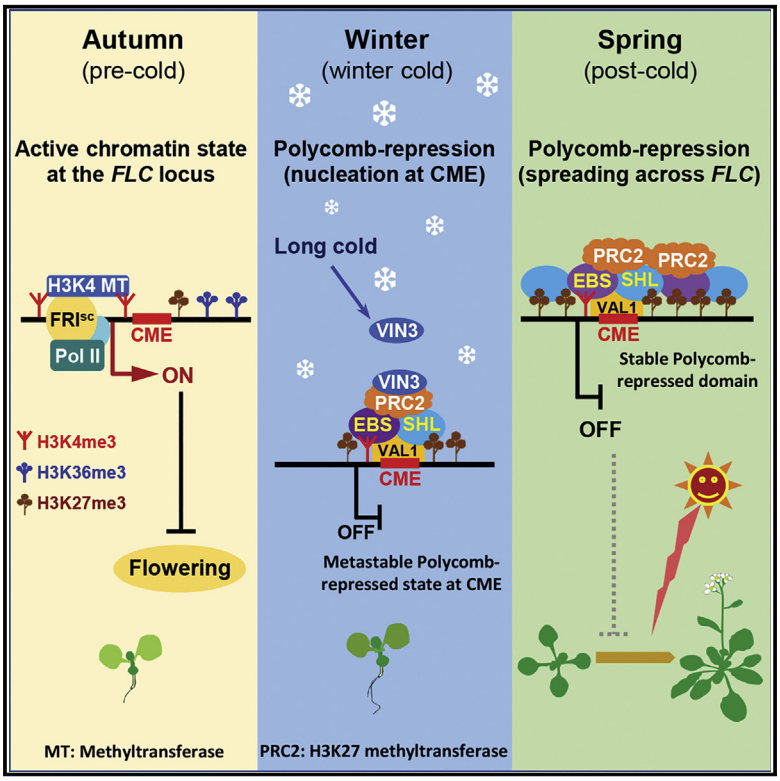

Highlights

- Cold memory element (CME) at *FLC* is associated with bivalent histone marks
- Dual histone readers (EBS and SHL) form dimers to read H3K4me3 and H3K27me3
- DNA-binding protein VAL1 recognizes CME and interacts with EBS and SHL
- CME-VAL1-EBS/SHL-PRC2 drives long cold-induced chromatin state switching

Authors

Zheng Gao, Yaxiao Li, Yang Ou, ..., Xiaolin Zeng, Renjie Li, Yuehui He

Correspondence

yhhe@pku.edu.cn

In brief

Gao et al. report that a 47-bp DNA element together with its associated bivalent chromatin feature at the floral repressor *FLC* drives the switching of an active chromatin state to Polycomb-repressed domain in response to prolonged cold exposure, which is stably maintained during post-cold growth and development to confer "memory of prolonged cold" in *Arabidopsis*.

Gao et al., 2023, Molecular Cell *83*, 1–16
April 6, 2023
https://doi.org/10.1016/j.molcel.2023.02.014

CellPress

Molecular Cell

CellPress

Article

A pair of readers of bivalent chromatin mediate formation of Polycomb-based "memory of cold" in plants

Zheng Gao,[1,3,4,5] Yaxiao Li,[3,5] Yang Ou,[1] Mengnan Yin,[1,3] Tao Chen,[3,6] Xiaolin Zeng,[1,3,7] Renjie Li,[1] and Yuehui He[1,2,3,8,*]

[1]State Key Laboratory of Protein and Plant Gene Research, Peking-Tsinghua Center for Life Sciences, School of Advanced Agricultural Sciences, Peking University, Beijing 100871, China

[2]Peking University Institute of Advanced Agricultural Sciences, Weifang, Shandong 261325, China

[3]Shanghai Center for Plant Stress Biology, CAS Center for Excellence in Molecular Plant Sciences, Chinese Academy of Sciences (CAS), Shanghai 201602, China

[4]University of Chinese Academy of Sciences, Beijing 100049, China

[5]These authors contributed equally

[6]Present address: Guangzhou KingMed Transformative Medicine Institute Co. Ltd., Guangzhou, Guangdong 510005, China

[7]Present address: Department of Chemistry, The University of Chicago, Chicago, IL 60637, USA

[8]Lead contact

*Correspondence: yhhe@pku.edu.cn

https://doi.org/10.1016/j.molcel.2023.02.014

SUMMARY

The Polycomb-group chromatin modifiers play important roles to repress or switch off gene expression in plants and animals. How the active chromatin state is switched to a Polycomb-repressed state is unclear. In *Arabidopsis*, prolonged cold induces the switching of the highly active chromatin state at the potent floral repressor *FLC* to a Polycomb-repressed state, which is epigenetically maintained when temperature rises to confer "cold memory," enabling plants to flower in spring. We report that the *cis*-acting cold memory element (CME) region at *FLC* bears bivalent marks of active histone H3K4me3 and repressive H3K27me3 that are read and interpreted by an assembly of bivalent chromatin readers to drive cold-induced switching of the *FLC* chromatin state. In response to cold, the 47-bp CME and its associated bivalent chromatin feature drive the switching of active chromatin state at a recombinant gene to a Polycomb-repressed domain, conferring cold memory. We reveal a paradigm for environment-induced chromatin-state switching at bivalent loci in plants.

INTRODUCTION

Polycomb-group (PcG) proteins introduce repressive chromatin modifications and implement transcriptional silencing in organisms from plants to humans.[1] In the crucifer plants such as *Arabidopsis thaliana*, prolonged cold exposure induces PcG-mediated chromatin silencing of the potent floral repressor *FLOWERING LOCUS C* (*FLC*; encoding a MADS-box transcription factor) to switch an active chromatin state to a Polycomb-repressed state in a physiological process termed vernalization (perception and "remembering of prolonged cold in winter").[2–4] This PcG-repressed state is epigenetically maintained through cell divisions when the temperature increases, resulting in stable *FLC* repression and conferring epigenetic memory of cold to enable the plants to flower under temperature favorable for seed production.[2,5]

Before cold exposure, the *FLC* expression is strongly upregulated by the plant-unique scaffold fold protein FRIGIDA (FRI) in association with active chromatin modifiers including several histone methyltransferases.[6,7] The histone 3 lysine-4 (H3K4) methyltransferase complex known as COMPASS-like and a histone 3 lysine-36 (H3K36) methyltransferase deposit H3K4 trimethylation (H3K4me3) in 5′ transcribed region encompassing the transcription start site (TSS) and H3K36 trimethylation (H3K36me3) in gene body at *FLC*, respectively, resulting in a highly activated chromatin state to activate *FLC* expression and thus prevent the floral transition.[6,7] On cold exposure, FRI proteins are sequestered into condensates, and *FLC* transcription is shut down in individual cells[8]; in addition, the expression of *VERNALIZATION INSENSITIVE 3* (*VIN3*), encoding a PLANT HOMEODOMAIN (PHD) finger protein, is gradually induced along prolonged cold.[9] VIN3, together with VIN3 LIKE 1 (VIL1)/VERNALIZATION 5 (VRN5), joins a pre-existing core PRC2 (consisting of an H3K27 methyltransferase and three structural subunits) to form the cold-specific VIN3 (PHD)-PRC2 with elevated catalytic activity to deposit repressive H3K27me3 at *FLC*.[10,11]

Please cite this article in press as: Gao et al., A pair of readers of bivalent chromatin mediate formation of Polycomb-based "memory of cold" in plants, Molecular Cell (2023), https://doi.org/10.1016/j.molcel.2023.02.014

VIN3-PRC2 is specifically enriched within a three-nucleosome region located in 5′ transcribed region and centered around the junction of the first exon/intron of *FLC*, resulting in H3K27me3 accumulation specifically in this region in cold,[12] but how VIN3-PRC2 is targeted to this region is unknown. Within this three-nucleosome region, there is a 47-bp *cis*-acting cold memory element (CME),[5] and two homologous *trans*-acting B3-domain proteins VP1/ABI3-LIKE 1 (VAL1) and VAL2 form dimers that recognize two 6-bp motifs in CME to promote cold-mediated *FLC* silencing.[5,13]

H3K27me3 is spread across the whole *FLC* gene body when temperature increases to normal.[14] As the spreading originates from the three-nucleosome region in 5′ *FLC*, this region is termed the "Polycomb nucleation region."[12] The spreading of H3K27me3 (to establish a Polycomb-repressed domain) and maintenance of this domain through cell divisions in subsequent growth and development confer cold memory in warmth.[12,14] In the warm, the VIN3 protein is rapidly degraded, but VIL1/VRN5 is relatively stable and remains to associate with the core PRC2 to mediate H3K27me3 spreading and maintenance at *FLC*.[3,15] VRN5-PRC2 couples with DNA replication during post-cold cell divisions to deposit H3K27 trimethylation at the canonical H3 variant H3.1 on *FLC* chromatin.[3,16] The H3K27me3 marks on *FLC* chromatin are partly recognized by LIKE HETEROCHROMATIN PROTEIN 1 (LHP1), which may function together with VRN5-PRC2 to maintain the cold-induced chromatin silencing of *FLC* in warmth[3,5]; however, *LHP1* appears to play a limited role because loss of *LHP1* function only causes a moderate *FLC* reactivation in the warm.[3] This suggests that there may exist other H3K27me3 readers critical for the maintenance of cold-induced Polycomb-repressed domain at *FLC*.

How the highly activated chromatin state at *FLC* is switched to a Polycomb-repressed domain has yet to be resolved, particularly regarding what defines the so-called Polycomb nucleation region as well as the paradoxical presence of the "activating" H3K4me3 marks in this region during and after cold exposure. Before cold, COMPASS (complex of proteins associated with Set1)-like deposits H3K4me3 in the 5′ transcribed *FLC* region, encompassing the region that subsequently functions as a Polycomb nucleation region on cold exposure.[7,17] During cold exposure, the level of H3K4me3 in the nucleation region seems to be reduced only moderately.[10,18] The role of these "active" H3K4me3 marks, if any, for cold-induced chromatin-state switching at *FLC* is essentially unknown.

The active mark H3K4me3 and repressive H3K27me3 can coexist in the same nucleosome or adjacent nucleosomes, resulting in bivalent chromatin regions or bivalent loci.[19,20] The balance between these two functionally opposite histone marks may enable fine transcriptional regulation of bivalent loci in response to developmental and external signals.[20,21] Bivalent chromatin regions are commonly found in mammalian embryonic stem cells and are often associated with loci poised for activation later in development or during differentiation.[19,20] In the *Arabidopsis* genome, several genome-wide profiling studies show that there are hundreds of loci that may bear H3K4me3 and H3K27me3 at a seedling stage,[22,23] but the role of bivalency in gene regulation is unclear in plants.

Histone marks are recognized specifically by readers. There are dual readers with two histone mark-binding domains to recognize distinct modifications.[24] Two plant-specific dual readers that recognize H3K4me3 and H3K27me3, EARLY BOLTING IN SHORT DAYS (EBS) and SHORT LIFE (SHL), have been characterized recently, and both readers are composed of a N-terminal bromo adjacent homology (BAH) to recognize H3K27me3, followed by a H3K4me3-binding PHD domain.[25–28] Both domains are required for *EBS* and *SHL* to regulate the expression of several examined target loci, and genome-wide profiling of EBS and SHL occupancy shows that most of the loci bound by EBS and/or SHL bear H3K4me3 or H3K27me3.[25–27] Furthermore, both EBS and SHL interact with the plant-specific Polycomb factor EMBRYONIC FLOWER 1 (EMF1) to form a BAH-EMF1 complex that mediates transcriptional repression.[25] Interestingly, structural analysis of EBS and SHL reveals that a single molecule of these dual readers only captures either H3K4me3 or H3K27me3, but not both, on H3 tails, due to the spatial constraint imposed by the proximity between the two histone mark-binding pockets[26,27]; hence, BAH-H3K27me3 and PHD-H3K4me3 binding from an EBS or SHL protein are independent and mutually exclusive. To date, whether EBS and SHL may read bivalent chromatin state is unknown.

Here, we report that EBS and SHL form homo- or hetero-dimers to function as chromatin bivalency readers that recognize H3K4me3 and H3K27me3 marks in the *cis*-acting CME region at *FLC* in the course of prolonged cold exposure to drive cold-induced switching of the active *FLC* chromatin state to a Polycomb-repressed state. Both EBS and SHL interact with VAL1 that recognizes CME and further nucleates the cold-specific VIN3-PRC2 in the bivalent CME region. After return to warmth, EBS and SHL are spread across the *FLC* locus and engage PRC2 for H3K27 trimethylation, resulting in the formation and maintenance of a Polycomb-repressed domain across *FLC* in post-cold growth and development, conferring cold memory.

RESULTS

The dual readers EBS and SHL function redundantly to mediate *FLC* silencing by prolonged cold

In response to prolonged cold exposure, the active H3K4me3-bearing chromatin state at *FLC* is switched to an H3K27me3-marked Polycomb-repressed domain. The dual readers of EBS and SHL can recognize both H3K4me3 and H3K27me3; hence, it was of interest to explore whether these readers may mediate cold-mediated *FLC* chromatin-state switching and consequent *FLC* repression. We first introduced loss-of-function *ebs* and *shl* alleles into a reference line of winter annuals (over-wintering accessions), Col-*FRI* (wild type [WT]), in which a functional *FRI* was introgressed into the rapid-cycling accession Col,[29] and subsequently, we followed *FLC* expression in the course of prolonged cold exposure, 35-day continuous cold. Without cold, *FLC* was expressed at similar levels among WT, *FRI ebs*, and *FRI ebs shl* seedlings but moderately lower in *FRI shl* (Figure 1A). Upon exposure to prolonged cold, *FLC* was repressed in *FRI shl* and further silenced after return to warmth, similar to WT,

Please cite this article in press as: Gao et al., A pair of readers of bivalent chromatin mediate formation of Polycomb-based "memory of cold" in plants, Molecular Cell (2023), https://doi.org/10.1016/j.molcel.2023.02.014

Molecular Cell
Article

Costrutti e point mutations

inducible VAL1 knock-down construct pER8-VAL1-amiRNA,

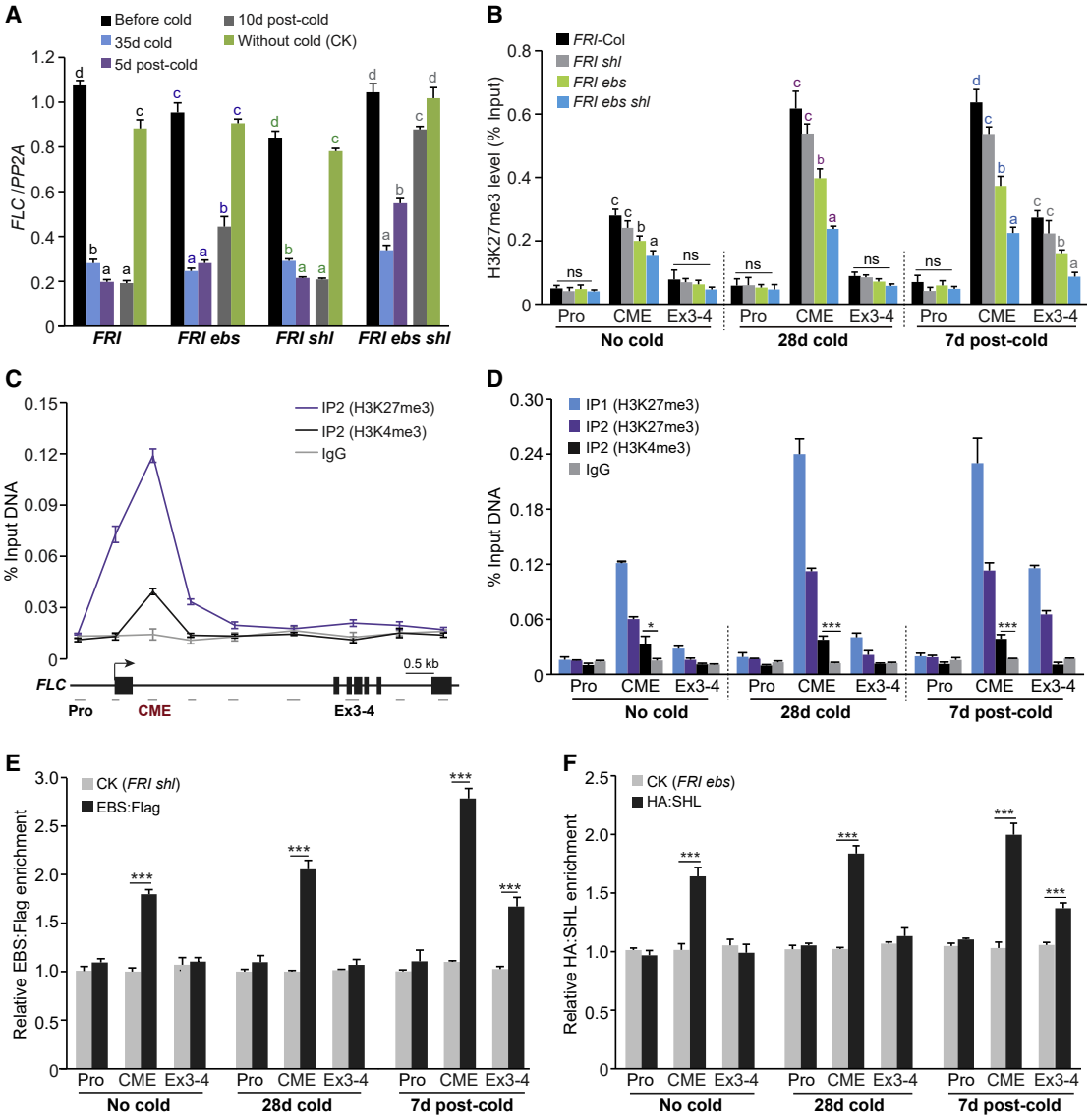

Figure 1. Polycomb-nucleating CME region at *FLC* possesses bivalent chromatin state read by EBS and SHL for cold-induced H3K27 trimethylation

(A) Mature *FLC* transcript levels in the indicated seedlings after 35-day continuous exposure to cold temperature. Data were measured by RT-qPCR and normalized to the reference gene *PROTEIN PHOSPHATASE 2A* (*PP2A*). "Without cold (CK)," non-vernalized plants at the development stage identical to the 10 days post-cold plants.

(B) ChIP-qPCR measurement of H3K27me3 at *FLC* in indicated seedlings after 28-day cold exposure. Levels of the immunoprecipitated fragments by anti-H3K27me3 were normalized to input DNA. 7 days post-cold, growth at normal temperature (22°C) for 7 days after cold. ChIP-examined regions are illustrated in (C).

(C and D) K27-K4 re-ChIP analysis of H3K4me3 and H3K27me3 on *FLC* chromatin. Levels of *FLC* fragments from anti-H3K27me3 and anti-H3K4me3 reChIP (using the seedlings cold-exposed for 28 days) were measured in (C), and additional samples were included in (D). IgG, reChIP with rabbit IgG as negative control. At bottom of (C) is a schematic drawing of the *FLC* locus; arrow for the transcription start site (TSS), and black boxes for exons and gray bars for the regions examined by ChIP.

(E and F) Enrichments of EBS (E) and SHL (F) at *FLC* after 28-day cold exposure. EBS:FLAG and HA:SHL are in the *FRI ebs shl* background. Levels of *FLC* fragments immunoprecipitated by anti-EBS:FLAG or anti-HA:SHL were normalized first to the internal control *SHOOT MERISTEMLESS* (*STM*),[18] and relative enrichments of EBS:FLAG or HA:SHL over a background control are calculated.

(A–F) Error bars denote standard deviation (SD) of three biological replicates. One-way ANOVA was conducted in (A) and (B) and letters in the same color denote statistically distinct means ($p < 0.01$), ns for not significant. Two-tailed t tests were conducted in (D)–(F); *$p < 0.05$, **$p < 0.01$, and ***$p < 0.001$.

See also Figures S1 and S2.

Please cite this article in press as: Gao et al., A pair of readers of bivalent chromatin mediate formation of Polycomb-based "memory of cold" in plants, Molecular Cell (2023), https://doi.org/10.1016/j.molcel.2023.02.014

whereas *FLC* expression in *FRI ebs* was moderately reactivated in the warm (Figure 1A). Interestingly, *FLC* expression was repressed in cold but fully reactivated in *FRI ebs shl* after 10-day growth in warmth (Figure 1A). Thus, *EBS* and *SHL* function redundantly and play an essential role to mediate *FLC* repression by prolonged cold.

We further measured flowering-time phenotypes of *FRI ebs*, *FRI shl*, and *FRI ebs shl* (hereinafter referred to as *ebs*, *shl*, and *ebs shl*, respectively), by scoring the total number of leaves formed before flowering. Without cold exposure, *ebs* and *shl* flowered moderately earlier than WT, whereas the double mutant flowered much earlier than WT (Figure S1A). It has been shown that *EBS* and *SHL* function in partial redundancy to repress the expression of *FLOWERING LOCUS T* (*FT*, encoding a major florigen) and inhibit the floral transition in rapid-cycling accessions.[25,28] We measured *FT* expression in these mutants (winter-annual background) and found that *FT* was strongly derepressed in *ebs shl* (Figure S1B), consistent with its early flowering-time phenotype. Next, we examined whether vernalization could accelerate the transition to flowering in *ebs shl* and found that it was completely insensitive to prolonged cold exposure (Figure S1A), consistent with the full post-cold *FLC* reactivation in this mutant.

EBS and *SHL* are essentially required for H3K27me3 accumulation in the CME region in cold and for its spreading on return to warmth

The loss of stable *FLC* repression in *ebs shl* in post-cold growth reflects the absence of H3K27me3-marked Polycomb-repressed state at *FLC*. To explore whether *EBS* and *SHL* are required to establish the H3K27me3 peak in the CME-bearing Polycomb nucleation region at *FLC* on prolonged cold exposure, we measured the levels of H3K27me3 at *FLC* on the functional loss of *EBS* and/or *SHL* by chromatin immunoprecipitation (ChIP) coupled with quantitative PCR. Before cold, H3K27 trimethylation occurred in the region encompassing CME but at low levels in the seedlings of WT, *shl*, *ebs*, and *ebs shl* (Figure 1B). Cold exposure resulted in a strong increase of H3K27me3 or H3K27me3 peak specifically in the CME region in the seedlings of WT and *shl*, but loss of *EBS* function led to a reduction in H3K27me3 accumulation (Figure 1B); moreover, the H3K27me3 peak was eliminated in *ebs shl*, that is, the level of H3K27me3 in the CME region in the cold-exposed double mutant was similar to that in WT (before cold) (Figure 1B). These results reveal that *SHL* and *EBS* function redundantly and with an essential role to promote H3K27 trimethylation in the CME-bearing Polycomb nucleation region in cold.

After 7 days of post-cold growth, we found that the H3K27 trimethylation in the CME region still requires *EBS* and *SHL* (Figure 1B). In addition, the spreading of H3K27me3 from the CME region to a distal gene-body region requires both *EBS* and *SHL*, as the simultaneous loss of *EBS* and *SHL* function eliminated H3K27me3 in this spreading site (Figure 1B). Thus, both *EBS* and *SHL* are required for spreading H3K27me3 from the CME region across the *FLC* locus in warmth. Taken together, these results reveal that *EBS* and *SHL* are essentially required for the establishment of the H3K27me3 peak in the CME region in cold and for its spreading across *FLC* in warmth and thus for switching the active *FLC* chromatin state to a Polycomb-repressed state.

EBS and SHL are enriched on *FLC* chromatin in the Polycomb-nucleation CME region in cold and post-cold

To uncover how EBS and SHL mediate cold-induced Polycomb repression at *FLC*, we first conducted ChIP to examine both proteins binding to *FLC* chromatin in the course of cold exposure, using transgenic seedings expressing functional tagged-EBS or SHL. There are two splice variants of EBS: EBS.1 and EBS.2 (with a shorter carboxyl-terminal loop than EBS.1).[25,27] We confirmed that EBS.2-FLAG was fully functional, whereas EBS.1-FLAG was partially functional (Figures S1C and S1D); thus, EBS.2-FLAG was used in subsequent experiments and referred to as EBS:FLAG. Before cold, the EBS:FLAG was moderately enriched specifically in the bivalent CME region, not in other regions at *FLC* (Figures 1E, S2A, and S2B), largely in line with the enrichment of EBS in 5′ transcribed *FLC* region, revealed by profiling of genome-wide binding sites of EBS.[25,27] We further found that prolonged cold led to an elevated enrichment of EBS:FLAG specifically in the CME region (Figure 1E). Similarly, SHL or the functional HA:SHL (Figure S1G) was moderately enriched specifically in the CME region before cold, and cold resulted in elevated binding to CME chromatin (Figures 1F, S2C, and S2D). During post-cold growth in warmth, the enrichments of both EBS and SHL were further elevated in the CME region (Figures 1E and 1F). Together, these results reveal that the dual readers of EBS and SHL bind the Polycomb-nucleation CME region; moreover, the similar patterns of temporal and spatial enrichment at *FLC* are well consistent with their redundant function in cold-induced *FLC* chromatin-state switching and *FLC* repression.

The CME region at *FLC* bears bivalent marks of H3K4me3 and H3K27me3

To determine how the dual histone readers of EBS and SHL bind CME chromatin, we first examined whether H3K4me3 and H3K27me3 may co-exist on the same or adjacent nucleosomes on part of *FLC* chromatin, using sequential ChIP (re-ChIP) of anti-H3K27me3 ChIP followed by ChIP with anti-H3K4me3 (designed as K27-K4 re-ChIP). We found that the CME region bore both H3K4me3 and H3K27me3 before cold, during prolonged cold exposure, and on return to warm, but these marks did not co-exist in other *FLC* regions (Figures 1C and 1D). Given the size of sheared DNA fragments in re-ChIP (about 150–500 bp with major bands of around 250 bp; see STAR Methods), these two marks were mainly from the CME-bearing nucleosome or adjacent nucleosomes. These results reveal that the regulatory CME region at *FLC* bears bivalent H3K4me3-H3K27me3 marks before cold exposure and remains bivalent during and after cold exposure.

EBS and SHL form homo- and hetero-dimer to read bivalent chromatin marks

Because of the spatial constraint imposed by the proximity between the histone mark-binding pockets in EBS and SHL, single proteins can bind only either H3K4me3 or H3K27me3.[26,27] We hypothesized that EBS and SHL may form a dimer to

Please cite this article in press as: Gao et al., A pair of readers of bivalent chromatin mediate formation of Polycomb-based "memory of cold" in plants, Molecular Cell (2023), https://doi.org/10.1016/j.molcel.2023.02.014

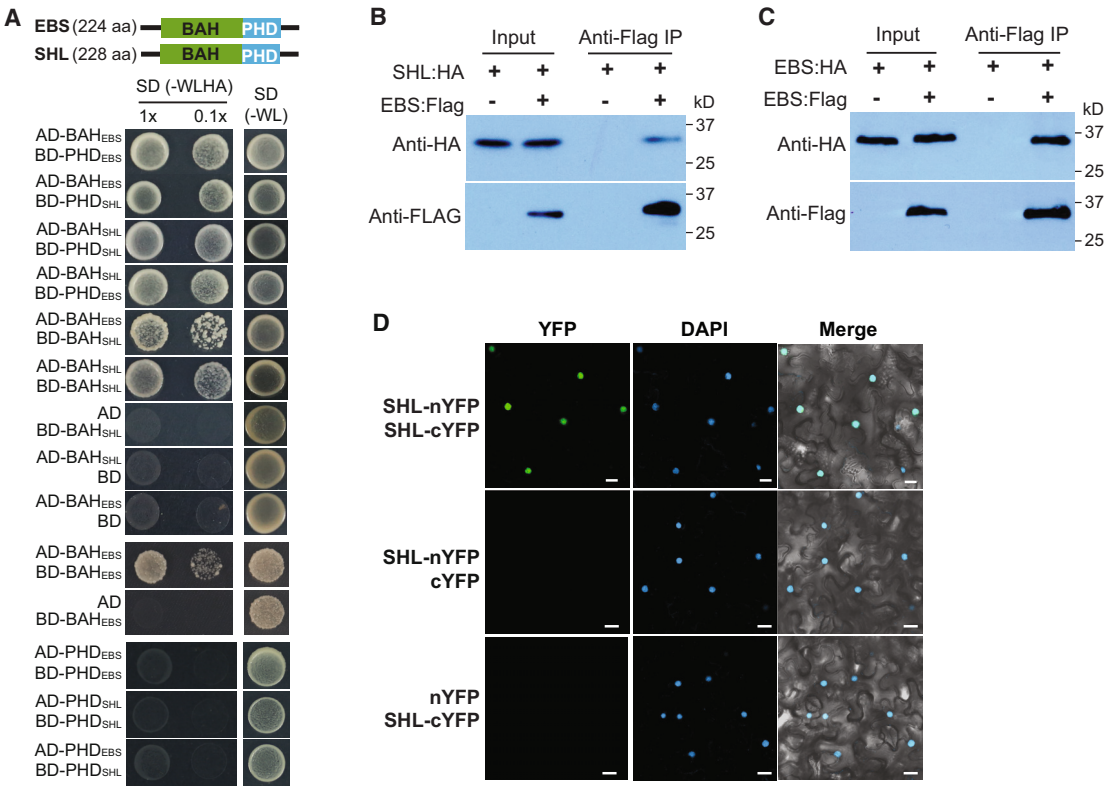

Figure 2. EBS and SHL form homo- and hetero-dimers

(A) Interactions of BAH-PHD and BAH-BAH from EBS and SHL in yeast cells. BAH and PHD domains were fused with the GAL4-AD or BD domain as indicated. 1× and 10× diluted yeast cells were spread on the highly stringent growth media of SD (-WLHA): without adenine (A), histidine (H), leucine (L), and tryptophan (W). Colonies on SD (-WL) serve as growth control.

(B and C) Coimmunoprecipitations (coIP) of EBS with SHL (B) and EBS (C). Total proteins from the F_1 seedlings expressing the indicated pair of proteins were subject to immunoprecipitation with anti-FLAG, followed by western blotting.

(D) BiFC analysis of self-interaction of SHL in *Nicotiana benthamiana* epidermal cells. Scale bars, 20 μm. For dimers' function, see also Figures S3 and S4.

simultaneously read the bivalent marks on the same or adjacent nucleosomes around CME and in other bivalent regions in the *Arabidopsis* genome. First, we tested whether these proteins could interact in yeast cells and found that the BAH domains from EBS and SHL interacted with itself and each other and with the PHD domains, but there was no interaction between PHD_{EBS} and PHD_{SHL} (Figure 2A). These results suggest that EBS and SHL form homo- or hetero-dimer through BAH-BAH or BAH-PHD interaction.

Next, we conducted coimmunoprecipitation (coIP) assays to confirm whether there are EBS-EBS and EBS-SHL associations in *Arabidopsis*, using F_1 seedlings expressing functional EBS:FLAG and EBS:HA (Figures S1D and S1E) or EBS:FLAG and SHL:HA[25] and found that EBS indeed associated with itself or SHL in *Arabidopsis* (Figures 2B and 2C). Moreover, bimolecular fluorescence complementation (BiFC) assays by transient co-expression of SHL-nYFP and SHL-cYFP in tobacco epidermal cells revealed that SHL physically interacted with itself in the nucleus (Figure 2D). Thus, EBS and SHL form homo- and hetero-dimers, which conceptually are able to simultaneously capture H3K4me3 and H3K27me3 from the same or adjacent nucleosomes in CME and other bivalent regions.

To investigate whether the assemblies of EBS and/or SHL are general readers of bivalent regions, we examined the enrichment of EBS and SHL at eight bivalent loci, selected and validated from a list of loci bearing H3K4me3 and H3K27me3 at an early seedling stage (Figures S3A and S3B). At seven of the eight bivalent loci, EBS and/or SHL specifically bind to the bivalent regions (Figures S4A and S4B), suggesting that EBS and SHL are general readers of the bivalent regions in *Arabidopsis*.

Binding of EBS and SHL to bivalent CME chromatin requires both BAH and PHD domains

EBS and SHL are composed of an H3K27me3-binding BAH domain followed by an H3K4me3-binding PHD domain; hence, we explored whether EBS and SHL bind bivalent CME chromatin via both BAH-H3K27me3 and PHD-H3K4me3. First, we created *SHL* transgenes with point mutations, in which two critical residues (W63L/Y65A) for H3K27me3 binding in the BAH domain or two key residues (F141A/Y148A) for H3K4me3 binding in the PHD domain were mutated[26]; in addition, a key residue in the BAH (P41L) or PHD domain (Y155A) was mutated in EBS.[25,27] These transgenes were introduced into *ebs shl*, and two independent single-locus lines for each transgene were further

Please cite this article in press as: Gao et al., A pair of readers of bivalent chromatin mediate formation of Polycomb-based "memory of cold" in plants, Molecular Cell (2023), https://doi.org/10.1016/j.molcel.2023.02.014

analyzed (Figures S1F and S1G). Previously, it has been shown that $SHL_{W63L/Y65A}$ binds to H3K4me3, but not to H3K27me3, whereas $SHL_{F141A/Y148A}$ binds to H3K27me3, but not to H3K4me3.[26] Using histone peptide pull-down assays, we confirmed that EBS_{P41L} binds to H3K4me3, but not to H3K27me3, whereas EBS_{Y155A} binds to H3K27me3, but not to H3K4me3 (Figure S5A). In addition, we confirmed that these mutations in BAH and PHD domains had no effect on BAH-BAH/PHD interactions (Figure S5B).

Next, we found that although EBS_{P41L}, EBS_{Y155A}, $SHL_{W63L/Y65A}$, and $SHL_{F141A/Y148A}$, tagged by FLAG or HA, all were expressed at levels similar to the fully functional EBS:FLAG or HA:SHL (Figures S5C and S5D), these point mutants (in *ebs shl*) were only partial functional compared with respective single mutants (Figures S1F, S1G, and S5E–S5G). We further found that *FLC* expression was reactivated after return to warmth, on a functional loss of BAH or PHD in either EBS or SHL (Figures 3A and 3D), suggesting that both BAH-H3K27me3 and PHD-H3K4me3 are required for cold-mediated *FLC* repression.

Next, we examined the binding of EBS_{P41L}, EBS_{Y155A}, $SHL_{W63L/Y65A}$, and $SHL_{F141A/Y148A}$ to the bivalent CME region. Compared with the WT EBS protein, the enrichments of EBS_{P41L} and EBS_{Y155A} in the CME region were strongly reduced in the seedlings exposed to prolonged cold (in cold and post-cold) (Figures 3B, 3C, S6A, and S6B). Similarly, the binding of $SHL_{W63L/Y65A}$ and $SHL_{F141A/Y148A}$ to CME chromatin was strongly reduced on cold exposure (in cold and post-cold), compared with the SHL protein (Figures 3E and S6C). These results show that both BAH-H3K27me3 and PHD-H3K4me3 are required for EBS and SHL binding to the bivalent CME chromatin upon prolonged cold exposure.

EBS and SHL are spread from the CME region across the *FLC* locus on return to warmth

We have thus far found that the CME region remains bivalent after return to warmth and that both EBS and SHL bind to the bivalent CME chromatin through PHD-H3K4me3 and BAH-H3K27me3, not only in cold but also in warmth. The bivalency on *FLC* chromatin occurs only in the CME region/Polycomb nucleation region, but interestingly, we found that EBS and SHL were enriched moderately in the H3K27me3-marked middle *FLC* region (a spreading site) after 7 days post-cold growth (Figures 1E and 1F), which seemed to require both functional BAH and PHD domains (Figures 3B, 3C, and 3E).

The PHD domains from EBS and SHL are able to bind to H3K4me2 in *in vitro* peptide-binding assays, but genome-wide profiling of EBS- or SHL-bound sites suggests that both readers largely bind to H3K4me3 and/or H3K27me3-marked regions.[25–27] Notably, H3K4me3 occurs typically around the TSSs and 5′ transcribed regions, whereas H3K4 dimethylation occurs in gene bodies in the *Arabidopsis* genome.[22] To validate that H3K4me2 is not involved in the binding of EBS or SHL to middle *FLC*, we conducted ChIP to examine H3K4me2 on *FLC* chromatin in the course of cold treatment. Before cold, H3K4me2 was enriched in the CME region and across gene body regions at *FLC* (Figure S6D). Given that before cold neither EBS nor SHL binds to the *FLC* gene body regions except the CME region (Figures S2A and S2C), these two readers may not recognize the H3K4me2 marks on *FLC* chromatin. We further found that the levels of H3K4me2 in the CME region increased moderately after prolonged cold exposure and were similar among the seedlings of WT, *ebs*, *shl*, and *ebs shl* (Figure S6E), revealing that neither EBS nor SHL is involved in H3K4me2 reading and maintenance at *FLC*. In addition, we found that H3K4me2 was moderately enriched in middle *FLC* before cold and in cold, but not on return to warmth (Figure S6E). Thus, the stable binding of EBS and SHL to middle *FLC* after return to warmth indeed is not mediated by PHD-H3K4me2 (or PHD-H3K4me3), but by BAH-H3K27me3. Given that Polycomb factors typically spread in *cis* from a nucleation region,[30] we reasoned that the reductions in the spreading of EBS and SHL from CME to the middle of *FLC* conceptually are attributed to a strong reduction in the binding of EBS or SHL with a defective PHD domain to the nucleating CME region.

The CME reader VAL1 functions to promote EBS enrichment at CME in cold and its subsequent spreading on return to warmth

EBS and SHL are essential for cold-induced H3K27me3 accumulation in the Polycomb-nucleating CME region. We reasoned that EBS and SHL may function together with the CME readers VAL1 (and VAL2) to mediate *FLC* repression by prolonged cold. First, we found that both EBS and SHL were able to interact with VAL1 through their PHD domains (Figure 4A). Next, we performed coIP assays using the F_1 seedlings from a functional VAL1:FLAG line[5] crossed to EBS:HA or SHL:HA lines and found that both EBS and SHL were associated with VAL1:FLAG (Figures 4B and 4C).

We further examined whether EBS enrichment at *FLC* is partly dependent on VAL1. On the loss of *VAL1* function, EBS:FLAG enrichment in the bivalent CME chromatin was strongly reduced in cold and post-cold growth (Figures 4F and S7A); thus, the CME-binding VAL1 functions to recruit or stabilize EBS binding to CME chromatin, suggesting that the binding of EBS to CME chromatin is through multivalent interactions including BAH-H3K27me3, PHD-H3K4me3, and EBS-VAL1-CME. In addition, we found that EBS binding to the spreading site, mid-*FLC*, was greatly reduced in *val1* (Figure 4F), suggesting that the CME-binding VAL1 function to promote EBS spreading in *cis* from the nucleating CME region across *FLC*. We further explored whether EBS and SHL may act to promote VAL1 enrichment on CME chromatin. Upon functional loss of *EBS* and *SHL*, we found that the enrichment of VAL1:FLAG at the CME region was reduced moderately following cold exposure and in the warm (Figures 4G and S7B), suggesting that the EBS and SHL proteins bound to the bivalent CME chromatin partly stabilize VAL1 binding to CME, perhaps in a positive feedback manner.

The elevated VAL1 enrichment at CME and the dependence of EBS binding CME chromatin on VAL1 after return to warmth suggest that VAL1 may play a critical role to maintain cold-induced *FLC* repression in warmth. To address the role of *VAL1* in the warm, we knocked down *VAL1* expression (in an *FRI val2* background) specifically on return to warm (Figure 4H), using a β-estradiol inducible artificial microRNA approach. Indeed, on *VAL1* knockdown after return to warmth, the levels of H3K27me3 on *FLC* chromatin were reduced, whereas H3K4me3 in the CME region was increased, resulting in a reactivation of the *FLC* expression (Figures 4I, 4J, and S7E). Thus, *VAL1*

Please cite this article in press as: Gao et al., A pair of readers of bivalent chromatin mediate formation of Polycomb-based "memory of cold" in plants, Molecular Cell (2023), https://doi.org/10.1016/j.molcel.2023.02.014

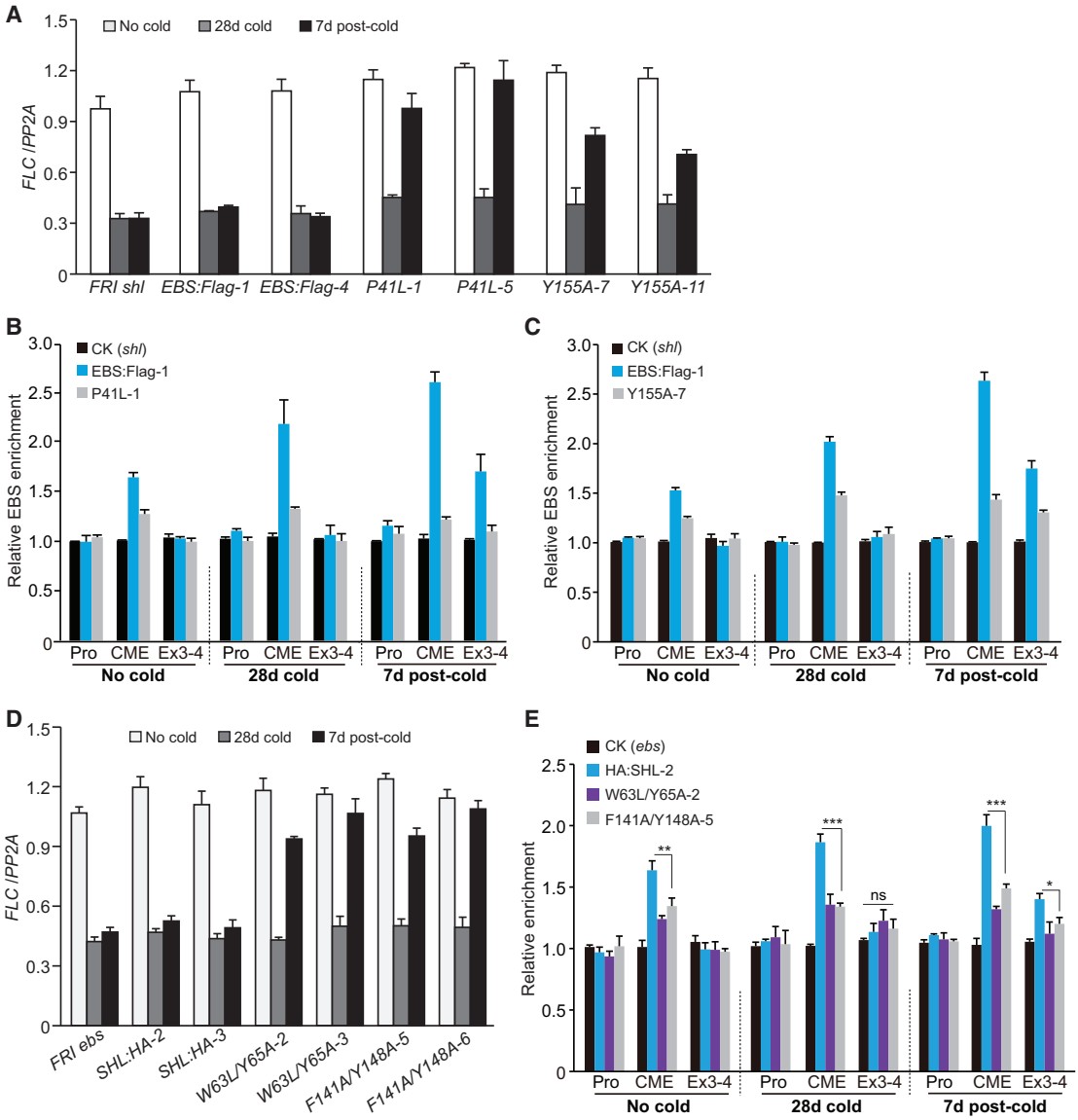

Figure 3. Functional analysis of BAH and PHD domains in EBS and SHL during cold-induced *FLC* repression

(A) Spliced *FLC* levels in the indicated seedlings cold-exposed for 28 days. Data were normalized to *PP2A*. *EBS:FLAG* (wild-type genomic *EBS.2* fused with FLAG) was introduced into *FRI ebs shl*, and *P41L* and *Y155A* are point-mutated *EBS:FLAG* genes. Two independent lines examined for each transgene.

(B and C) EBS_{P41L} (B) and EBS_{Y155A} (C) enrichments at *FLC*.

(D) Spliced *FLC* levels in the indicated seedlings. *HA:SHL* (wild-type genomic *SHL* fused with HA) was introduced into *FRI ebs shl*, and *W63L/Y65A* and *F141A/Y148A* are point-mutated *HA:SHL* genes. Two independent lines examined for each transgene.

(E) Enrichments of SHL, $SHL_{W63L/Y65A}$, and $SHL_{F141A/Y148A}$ at *FLC*.

(B, C, and E) Levels of *FLC* fragments immunoprecipitated by anti-FLAG or anti-HA were normalized first to the internal control *STM*, and relative enrichments of wild-type and mutated EBS:FLAG or HA:SHL over a background control (CK) are calculated.

(A–E) Seedlings were exposed to cold for 28 days; error bars denote SD of three biological replicates.

See also Figures S1, S5, and S6.

is required not only for the establishment of the H3K27me3 peak in the Polycomb-nucleating CME region in cold but also for the formation and maintenance of the Polycomb-repressed domain at *FLC* through cell divisions during post-cold growth and development, consistent with the function of VAL1 in EBS spreading across *FLC*.

EBS and SHL interact with and engage the cold-induced VIN3 protein in the Polycomb-nucleating CME region

The cold-specific VIN3-PRC2 is essential for cold-induced H3K27me3 at *FLC*.[11] To explore how VIN3 is recruited to the nucleating CME region, we examined whether EBS and SHL may interact with VIN3. Previously, it has been shown that the

Please cite this article in press as: Gao et al., A pair of readers of bivalent chromatin mediate formation of Polycomb-based "memory of cold" in plants, Molecular Cell (2023), https://doi.org/10.1016/j.molcel.2023.02.014

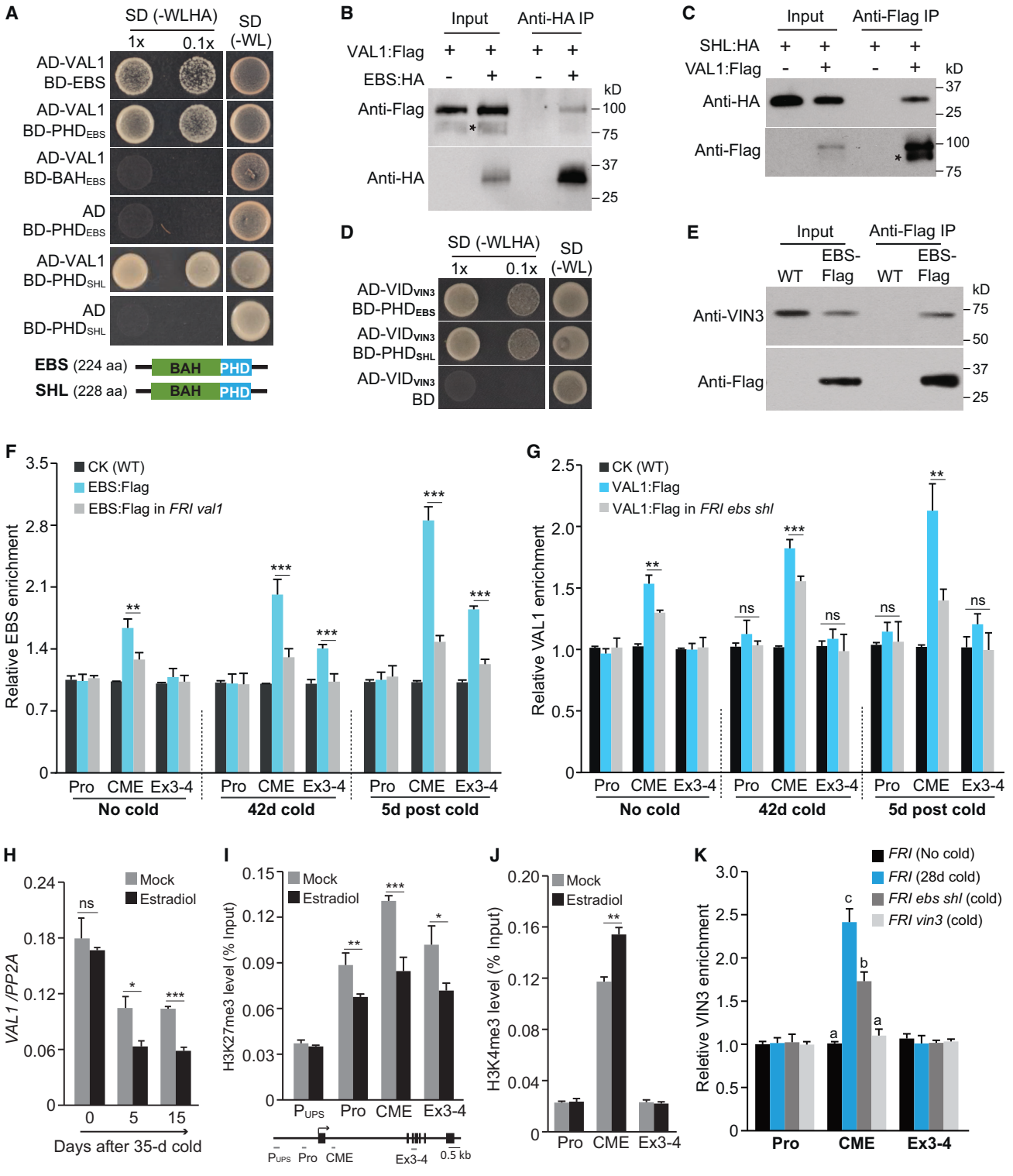

Figure 4. VAL1 interacts with EBS and SHL that nucleate the cold-specific VIN3-PRC2 in the CME region and regulates CME bivalency

(A) Both EBS and SHL interacted with VAL1 through their PHD domains in yeast cells, as indicated by the colonies grown on the highly stringent SD (-WLHA) media.

(B and C) CoIP of VAL1 with EBS (B) and SHL (C). Total proteins from the F_1 seedlings expressing EBS:HA or SHL:HA with VAL1:FLAG were subjected to immunoprecipitations by anti-HA beads. Asterisks denote a degradation product of VAL1:FLAG.

(legend continued on next page)

Please cite this article in press as: Gao et al., A pair of readers of bivalent chromatin mediate formation of Polycomb-based "memory of cold" in plants, Molecular Cell (2023), https://doi.org/10.1016/j.molcel.2023.02.014

plant-specific VIN3 INTERACTING DOMAIN (VID) mediates interactions of VIN3 with itself and VIL1/VRN5.[31,32] We found that the VID domain from VIN3 was able to interact with the PHD domains from both EBS and SHL (Figure 4D), and subsequent coIP assays using cold-treated *EBS:FLAG* seedlings and a rabbit polyclonal anti-VIN3 revealed that VIN3 was immunoprecipitated by anti-FLAG (EBS:FLAG) (Figures 4E and S7C). Thus, VIN3 indeed associates with EBS in cold-treated seedlings.

Next, we examined the enrichment of cold-induced VIN3 protein at *FLC* and found that it was enriched specifically at the CME region on prolonged cold exposure, but a functional loss of EBS and SHL caused a strong reduction (Figures 4K and S7C), revealing that these bivalent readers are required to recruit VIN3 or stabilize its binding at the CME region in cold. Taken together, these results suggest that the EBS and SHL proteins bound to the bivalent CME region engage the cold-specific VIN3-PRC2 for H3K27 trimethylation at *FLC*, resulting in the nucleation of Polycomb factors in the regulatory CME region during cold exposure.

Cold induces an elevation in H3K27me3 on the bivalent CME chromatin

Using sequential ChIP of K27-K4 (anti-H3K27me3 followed by anti-H3K4me3), we have found that CME chromatin is in the bivalent state before, during, and post cold exposure (Figure 1D). To determine whether cold-induced H3K27me3 by VIN3-PRC2 in the CME region may occur in H3K4me3-bearing nucleosomes, we further conducted sequential K4-K27 ChIP assays using WT and *ebs shl* seedlings. In WT, the level of H3K4me3 in the CME region was only moderately reduced on prolonged cold exposure and after return to warmth (Figure 5A). Interestingly, we observed that cold exposure caused a strong increase of H3K27me3 in the nucleosomes around CME immunoprecipitated by anti-H3K4me3 in WT (see ratios of H3K27me3 recovered in reChIP/IP2 to H3K4me3 in ChIP/IP1; Figure 5A). Thus, cold induces H3K27 trimethylation in the H3K4me3-bearing or adjacent nucleosomes around CME; furthermore, the active H3K4me3 marks in the Polycomb-nucleating CME region largely are not removed in the switching of *FLC* chromatin state in response to cold.

Next, we compared the levels of H3K4me3 and H3K27me3 at *FLC* between WT and *ebs shl*. Upon functional loss of EBS and SHL, the level of H3K4me3 in the CME region was moderately reduced prior to cold (Figures 5A and 5B), suggesting that these two H3K4me3 readers partly maintain this mark. Furthermore, there was no increase in H3K27me3 in the bivalent nucleosomes of the CME region in *ebs shl* (Figure 5B), consistent with that EBS and SHL are essential for cold-induced H3K27 trimethylation in the Polycomb nucleation region at *FLC*.

PHD-H3K4me3 recognition is required for cold-induced H3K27 trimethylation in the bivalent CME region

H3K4me3 is associated with active gene expression in eukaryotes and often functions to promote gene expression, and thus, it is termed an active or activating mark.[33,34] Prior to cold, the COMPASS-like H3K4 methyltransferase complex catalyzes H3K4me3 to activate *FLC* expression.[17] Interestingly, during cold-induced switching of *FLC* chromatin state, we have found that the PHD domains from EBS and SHL read and maintain the H3K4me3 marks in the bivalent CME region. Because both EBS and SHL interact with the VIN3 protein to promote H3K27me3 in the regulatory CME region in cold, the H3K4me3 marks in this region actually function to silence *FLC* expression in response to prolonged cold. Consistently, we found that in cold and after return to warmth, the levels of H3K27me3 in the CME region were reduced in the EBS_{Y155A} lines (in the *ebs shl* background) with a defective PHD domain unable to recognize H3K4me3, compared with the WT EBS lines (Figures 5C and S6F). Thus, H3K4me3 recognition by EBS is partly required for cold-induced H3K27 trimethylation in the bivalent CME region.

VIN3-PRC2-dependent H3K27 trimethylation promotes EBS binding CME chromatin in cold

Both PHD-H3K4me3 and BAH-H3K27me3 mediate the binding of EBS and SHL to the bivalent CME chromatin. We further validated the role of BAH-H3K27me3 recognition for cold-induced H3K27 trimethylation in the CME region and found that the P41L mutation in the BAH domain of EBS resulted in a loss of H3K27me3 in the CME region in cold (Figures 5D and S6G). Thus, the reading of H3K27me3 by EBS (and SHL) promotes the establishment of the H3K27me3 peak in the nucleating CME region in cold, which may in turn promote further binding of EBS and SHL to this region.

To elucidate the role of VIN3 (PRC2)-dependent H3K27 trimethylation for cold-regulation of EBS enrichment in the CME region, we modulated *VIN3* expression using a short cold-responsive promoter from *COLD REGULATED 78* (*COR78*).[35] On 14-day cold exposure, *VIN3* expression was greatly induced in the transgenic seedlings bearing *COR78pro-VIN3*, and consequently, EBS

(D) The VID domain of VIN3 interacted with PHD_{EBS} and PHD_{SHL} in yeast cells.
(E) CoIP of EBS with VIN3 in the *EBS:FLAG* seedlings cold-exposed for 28 days. Anti-FLAG immunoprecipitations were examined by western blotting with rabbit polyclonal anti-VIN3.
(F and G) Enrichments of EBS (F) and VAL1 (G) on *FLC* chromatin. The seedlings of *EBS:FLAG FRI val1*$^{+/-}$, *EBS:FLAG FRI val1* (E), *VAL1:FLAG FRI ebs*$^{+/-}$ *shl*$^{+/-}$, and *VAL1:FLAG FRI ebs shl* (F) were exposed to cold for 42 days. Levels of the *FLC* fragments from anti-FLAG ChIPs were normalized first to *STM*, and relative enrichments of EBS:FLAG and VAL1:FLAG over a background control are shown.
(H) Inducible knockdown of *VAL1* expression specifically on return to warm. *FRI val2* seedlings were applied daily with estradiol starting 2 days before return to warmth. Data were normalized to *PP2A*.
(I and J) Changes of H3K27me3 (I) and H3K4me3 (J) at *FLC*, on *VAL1* knockdown in the warm for 15 days. ChIP was conducted with newly emerged leaves.
(K) VIN3 enrichment in the CME region requires EBS and SHL in the seedlings cold-exposed for 28 days. Levels of *FLC* fragments from anti-VIN3 ChIP were normalized to *STM*, and relative VIN3 enrichments over a control (Col-*FRI* without cold) were shown.
(F–K) Error bars denote SD of three biological replicates. One-way ANOVA and two-tailed t test were conducted in (F), (G), and (K) and (H)–(J), respectively; ns for not significant, *$p < 0.05$, **$p < 0.01$ and ***$p < 0.001$.
See also Figure S7.

Please cite this article in press as: Gao et al., A pair of readers of bivalent chromatin mediate formation of Polycomb-based "memory of cold" in plants, Molecular Cell (2023), https://doi.org/10.1016/j.molcel.2023.02.014

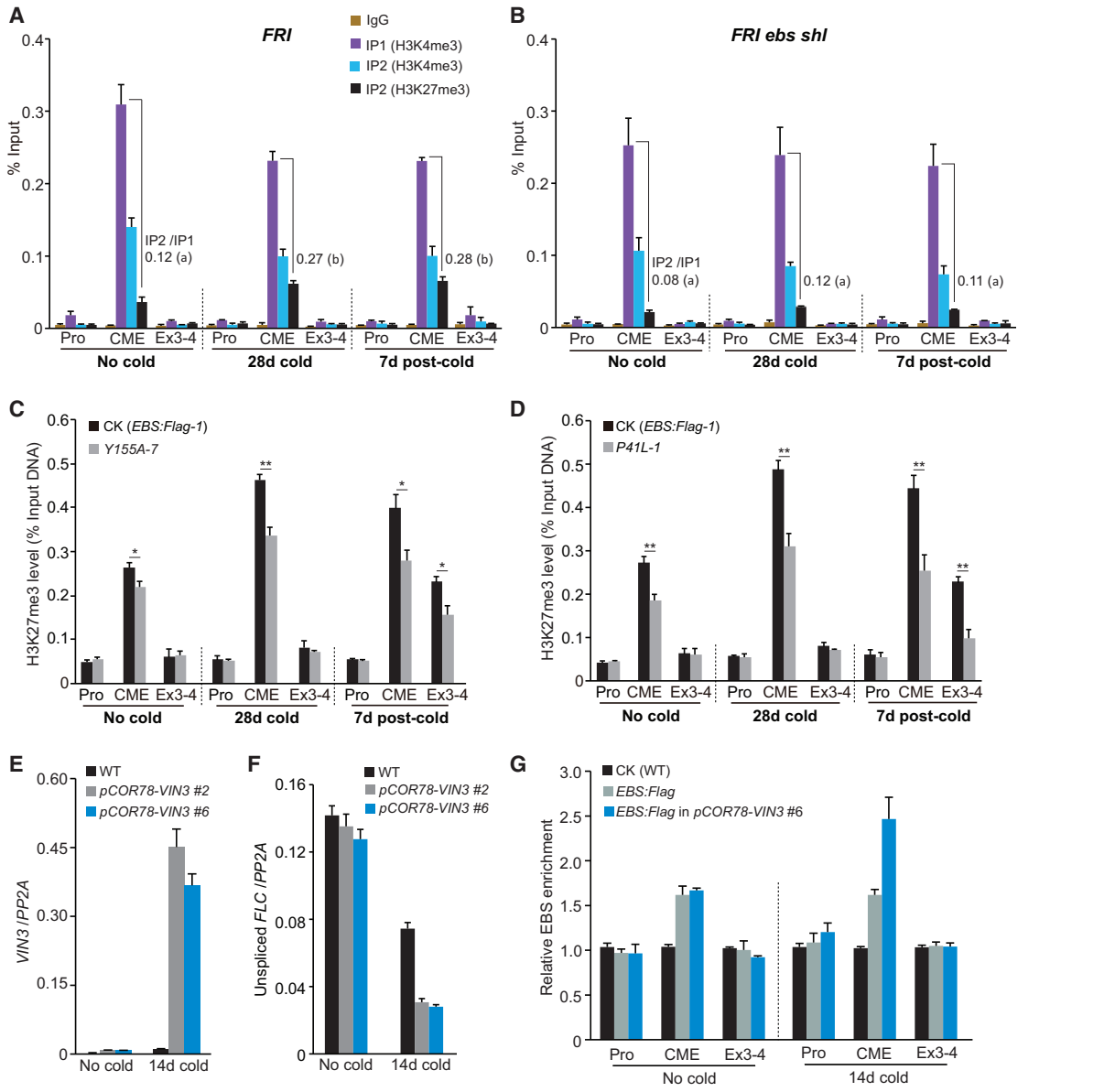

Figure 5. Cold-induced H3K27 trimethylation in the bivalent CME region requires functional coordination of EBS and VIN3

(A and B) Sequential H3K4me3-H3K27me3 re-ChIP assays on *FLC* chromatin in WT (A) and *ebs shl* (B) after 28-day cold exposure. Levels of the immunoprecipitated *FLC* fragments were normalized to input DNA. IgG, negative control. Average ratios of the level of H3K27me3 recovered from IP2 (reChIP) to H3K4me3 from IP1 are denoted, and letters in parentheses mark statistically significant differences (one-way ANOVA, $p < 0.01$).

(C and D) ChIP analysis of H3K27me3 at *FLC* in H3K4me3-binding defective EBS_{Y155A}-FLAG (C) or H3K27me3-binding defective EBS_{P41L}:FLAG (D). Data were analyzed by two-tailed t test; *$p < 0.5$ and **$p < 0.01$.

(E and F) Levels of mature *VIN3* mRNAs (E) and primary *FLC* mRNAs (F) in the indicated seedlings after 14-day cold exposure. Data were normalized to *PP2A*.

(G) Elevated EBS:FLAG enrichment on *CME* chromatin upon a strong *VIN3* induction by 14-day cold. Relative EBS:FLAG enrichments over a background control were shown.

(A–G) Error bars denote SD of three biological replicates.

See also Figure S6.

was greatly enriched in the CME region, resulting in a great transcriptional repression of *FLC* expression (Figures 5E–5G). Thus, VIN3-PRC2-dependent H3K27 trimethylation underlies cold promotion of the enrichment of EBS (and likely SHL) in the CME region.

Spreading of EBS and SHL mediates the formation of H3K27me3-marked Polycomb-repressed domain at *FLC*

Both EBS and SHL are spread from the nucleating CME region across *FLC* after cold. It was of interest to explore how EBS and SHL mediate H3K27me3 spreading. VIN3 is rapidly degraded

Please cite this article in press as: Gao et al., A pair of readers of bivalent chromatin mediate formation of Polycomb-based "memory of cold" in plants, Molecular Cell (2023), https://doi.org/10.1016/j.molcel.2023.02.014

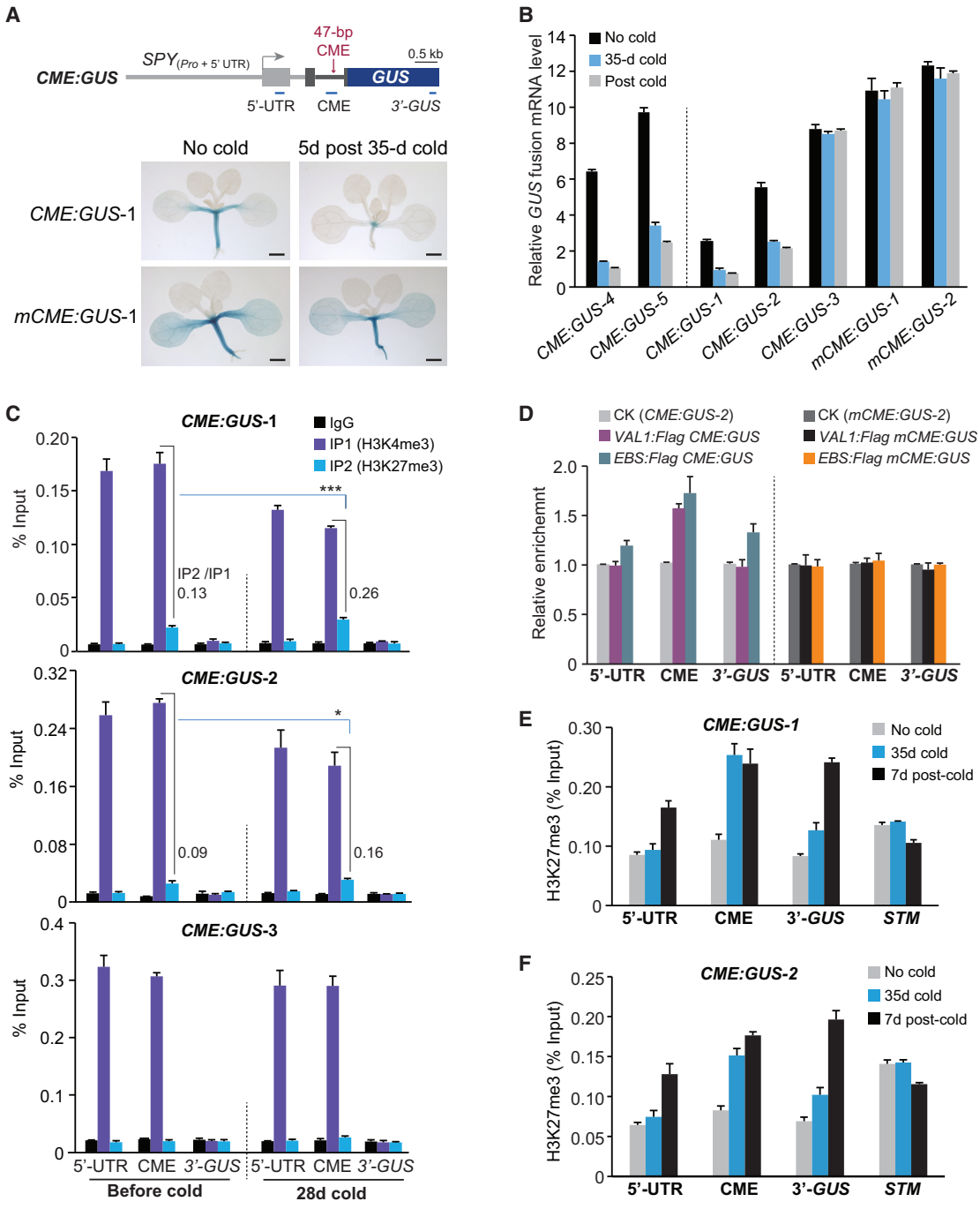

Figure 6. Bivalent CME drives switching of an active chromatin state to a stable Polycomb-repressed domain at the recombinant gene *CME:-GUS*, in response to prolonged cold

(A) Histochemical GUS staining. Scale bars, 1 mm. On top is a schematic drawing of *CME:GUS* with a promoter region from the constitutively expressed *SPINDLEY* (*SPY*, At3G11540)[5]; the gray arrow for TSS, filled boxes for exons, and blue bars for ChIP-examined regions.

(B) Levels of unspliced *CME:GUS* transcripts in the indicated seedlings after 35-day cold. Data were normalized to unspliced *PP2A*. Seedlings were sampled immediately after cold, and 5 days or 7 days post-cold. Error bars denote SD of three biological replicates except for *CME*:GUS-4 and -5 with two replicates.

(C) Re-ChIP analysis of *CME:GUS* chromatin bivalency in the indicated seedlings. IgG, negative control. Average ratios of the level of H3K27me3 recovered from IP2 to H3K4me3 from IP1 are denoted and analyzed by two-tailed t test (*$p < 0.05$ and ***$p < 0.001$).

(D) Enrichments of VAL1:FLAG and EBS:FLAG on *CME:GUS* chromatin upon 35-day cold exposure. F_1 seedlings from crossing *VAL1:FLAG* and *EBS:FLAG* to *CME*:GUS-2 or *mCME*:GUS-2 were harvested right after cold.

(legend continued on next page)

Please cite this article in press as: Gao et al., A pair of readers of bivalent chromatin mediate formation of Polycomb-based "memory of cold" in plants, Molecular Cell (2023), https://doi.org/10.1016/j.molcel.2023.02.014

when the temperature increases, but VRN5 is relatively stable in the warm, and the remaining VRN5-bearing PRC2 (VRN5-PRC2) catalyzes H3K27me3 across *FLC* chromatin.[3] We found that the VID domain in VRN5, like that in VIN3, interacted with the PHD domains of EBS and SHL (Figure S7D), suggesting that during post-cold spreading of PRC2, EBS, and SHL, these factors function in concert to mediate H3K27 trimethylation across *FLC*. Consistently, we found that after return to warmth, H3K27 trimethylation in a spreading site (middle *FLC*) or H3K27me3 spreading was nearly eliminated in *ebs shl* (Figure 1B). As BAH-H3K27me3 stabilizes the binding of EBS and SHL over H3K27me3-spreading regions, these readers and VRN5-PRC2 conceptually mediate H3K27me3 spreading in a positive feedback manner. Consistent with this notion, the lack of H3K27me3 binding by EBS_{P41L} (in *ebs shl*) led to a near elimination of H3K27 trimethylation in the middle *FLC* region after cold, thus disabling H3K27me3 spreading (Figures 5D and S6G). In short, the spreading of EBS and SHL mediates the formation of H3K27me3-marked Polycomb-repressed domain at *FLC*, resulting in its chromatin-state switching in response to prolonged cold.

Bivalent CME drives chromatin-state switching to confer the epigenetic memory of cold at a recombinant gene in response to cold

We have thus far found that EBS and SHL read the bivalency of Polycomb-nucleating CME region to drive chromatin-state switching at *FLC* and thus confer *FLC* repression in response to prolonged cold. Next, we explored whether the bivalent CME is sufficient to drive chromatin-state switching, using a recombinant reporter gene without any *FLC* sequence except for the 47-bp CME to exclude probable involvement of any long non-coding RNAs (lncRNAs) from the *FLC* locus.[36] In this recombinant gene, the 5′ end of *β-GLUCURONIDASE* (*GUS*) reporter gene is fused with a reconstructed exon-intron-exon cassette from a gene lacking CME, driven by a constitutive promoter, and CME is inserted in an intron upstream of *GUS* (hereinafter referred to as *CME:GUS*).[5] We randomly selected five independent single-locus *CME:GUS* transgenic lines and two lines of the recombinant *GUS* gene with the insertion of a mutated *CME* (*mCME:GUS*, replacing TGCATG with CTTGAC[5]) for cold treatment. Subsequently, we found that the expression of *GUS* fusion gene was repressed in cold as well as after return to warmth in four of the five *CME:GUS* lines, whereas in the remaining line (*CME*:GUS-3), it was not repressed, like that in the two *mCME:GUS* lines (Figures 6A and 6B). Thus, CME alone is insufficient to confer cold-induced repression, and likely, the chromatin feature of *CME:GUS* plays an important role in its repression by prolonged cold, as the chromatin feature of the transgene in *CME*:GUS-3 may be different from that in the rest of four lines, owing to a potential positional effect at the chromosomal integration site of the transgene.

The bivalency of the Polycomb-nucleating CME region at *FLC* has been shown to be critical for prolonged cold-mediated *FLC* repression; hence, we examined the bivalency of the CME region of *CME:GUS* in the five transgenic lines during the course of cold treatment by sequential K4-K27 ChIP. Before cold, the CME regions in all five transgenes were enriched with the active H3K4me3 marks, consistent with active transcription of the *GUS* fusion (Figures 6B, 6C, S7G, and S7H). Interestingly, the H3K4me3-marked CME chromatin from the four lines with cold-responsive *CME:GUS* also bore low levels of H3K27me3, but this bivalency did not occur in *CME*:GUS-3 (Figures 6C, S7G, and S7H). On prolonged cold exposure, CME chromatin remained bivalent with an apparent elevation in H3K27me3 in the four cold-responsive *CME:GUS* lines, whereas in the cold-insensitive *CME*:GUS-3 line, the CME region remained being only with H3K4me3 (Figures 6C, S7G, and S7H). These results suggest that the *cis*-acting CME together with its bivalent chromatin feature confer cold-mediated repression of *CME:GUS*.

We further examined the binding of VAL1 and EBS to *CME:GUS* chromatin and found that on long cold exposure, both VAL1 and EBS were enriched in the CME region (Figure 6D). Thus, similar to the situation at *FLC*, the regulatory module of CME-VAL1-EBS confers cold-mediated *CME:GUS* repression. Next, we followed H3K27me3 states on *CME:GUS* chromatin in two cold-responsive lines in the course of cold exposure and found that cold-induced H3K27me3 accumulation at the CME region and that after 7 days of post-cold growth, H3K27me3 was spread from the nucleating CME region to cover the entire *CME:GUS* transgene (Figures 6E and 6F), resulting in a Polycomb-repressed domain and thus switching of the active chromatin state to Polycomb-repressed at *CME:GUS*. Taken together, these results reveal that in response to prolonged cold, bivalent CME drives chromatin-state switching and confers a Polycomb-repressed domain and cold memory at the recombinant *GUS* fusion gene. This provides compelling evidence that the *cis*-acting CME at *FLC* together with its associated bivalent chromatin feature drive the cold-induced chromatin-state switching and confer epigenetic memory of cold in *Arabidopsis*.

DISCUSSION

We have discovered that the readers of bivalent chromatin EBS and SHL as well as the bivalency of the Polycomb-nucleating CME region are the long-sought elements in the cold-induced chromatin state switching and the formation of epigenetic "memory of winter cold" in *Arabidopsis*. EBS and SHL read and interpret the bivalency of the regulatory CME region, function essentially for nucleating PcG factors and H3K27 trimethylation in this region in cold, and for subsequent post-cold H3K27me3 spreading and formation of the Polycomb-repressed domain across *FLC* (Figure 7).

Our results show that the 47-bp CME together with its bivalent chromatin feature drive chromatin-state switching in response to cold and mediate the maintenance of Polycomb-repressed domain at a recombinant gene through cell divisions. The

(E and F) ChIP analysis of H3K27me3 at *CME:GUS* in the indicated seedlings after 35-day cold. Levels of the indicated DNA fragments were normalized to input DNA. Note that there was no cold-induced elevation of H3K27me3 at the endogenous H3K27me3-bearing *STM*.
(C–F) Error bars denote SD of three biological replicates.
See also Figure S7.

Please cite this article in press as: Gao et al., A pair of readers of bivalent chromatin mediate formation of Polycomb-based "memory of cold" in plants, Molecular Cell (2023), https://doi.org/10.1016/j.molcel.2023.02.014

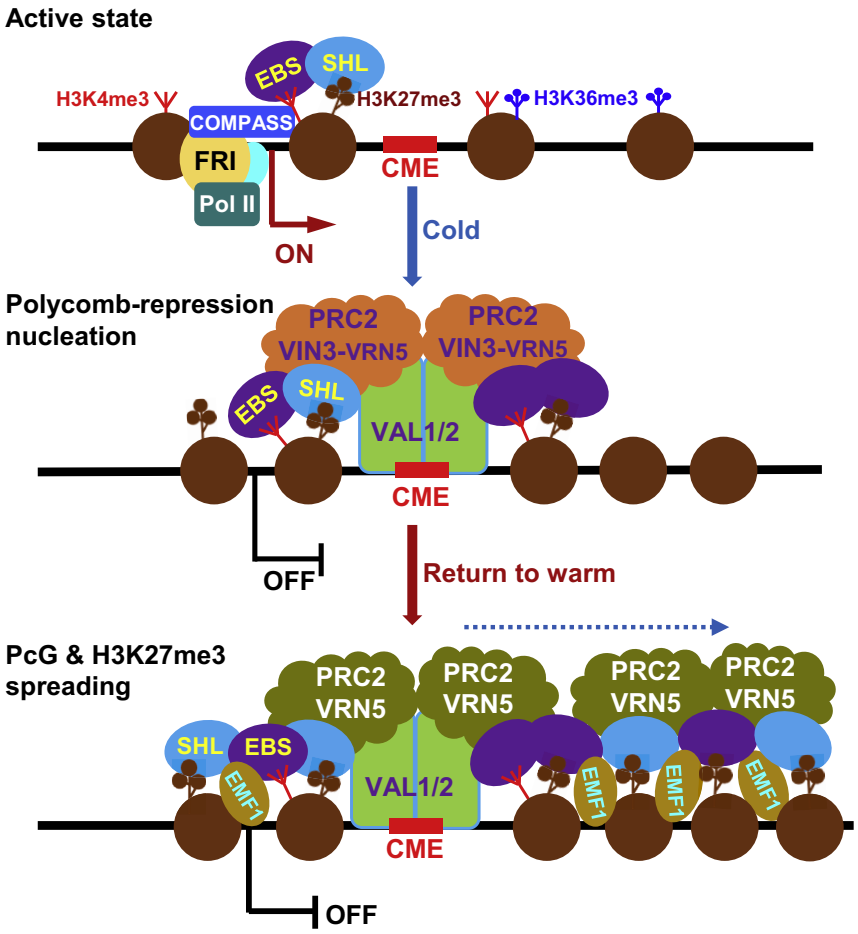

Figure 7. Working model for the cold-induced chromatin-state switching at *FLC*

Prior to cold, COMPASS-like and other modifiers deposit active H3K4me3 and H3K36me3 for a highly activated *FLC* chromatin state with the bivalent CME region (encompassed by two nucleosomes) read by a low level of EBS and SHL. Along prolonged cold, *FLC* transcription is shut down, and VAL1 and VAL2 specifically recognize CME and are increasingly enriched; in addition, EBS and SHL, through BAH-H3K27me3, PHD-H3K4me3, and association with VAL1/2-CME, are increasingly enriched and further nucleate the cold-specific VIN3-PRC2 in the CME region. This results in H3K27me3 accumulation in the nucleating CME region in cold, which in turn promotes EBS and SHL enrichment. After return to warm, VIN3 is rapidly degraded, and EBS, SHL, and VRN5-PRC2 are spread to mediate H3K27me3 spreading across the *FLC* locus, in a positive feedback manner, which antagonizes H3K36 trimethylation across the gene body. Furthermore, EBS and SHL associate with EMF1 to mediate chromatin compaction for transcriptional repression.[25] These molecular events lead to the formation and maintenance of a stable Polycomb-repressed domain at *FLC*, conferring epigenetic memory of cold in the warmth. Notably, PRC2 dimerizes for efficient H3K27 trimethylation,[37] and given the homo- and hetero-interaction of VIN3 and VRN5, the PRC2s at *FLC* may function as dimers for efficient H3K27 trimethylation.

findings from *FLC* and the CME-bearing recombinant gene reveal that CME (DNA sequence)-specific recruitment of Polycomb factors (VIN3/VRN5-PRC2) via VAL1 and EBS/SHL is essential for the formation and subsequent maintenance of cold-induced Polycomb-repressed chromatin at *FLC* through cell divisions in *Arabidopsis*. Interestingly, it has been shown in *Drosophila* that maintenance of Polycomb-repressed chromatin through cell divisions requires DNA sequence-specific recruitment of Polycomb factors.[38,39] Similarly, in *Schizosaccharomyces pombe*, a DNA sequence-dependent mechanism is required for the inheritance of H3K9 trimethylation-marked heterochromatin,[40] and a 147-bp DNA sequence of "maintainer" is sufficient for the epigenetic inheritance of heterochromatin through cell divisions.[41] These findings suggest that *cis*-acting DNA elements play a general role in epigenetic inheritance of Polycomb-repressed domains and heterochromatin in fungi, plants, and animals.

Prolonged cold induces the establishment of a Polycomb-repressed domain at *FLC*. In *de novo* formation of the Polycomb-repressive domain in mammals, Polycomb factors (e.g., PRC2) stably bind to the nucleation region first and are subsequently spread in *cis* to proximal regions.[30] Similarly, both EBS and SHL, highly enriched in the nucleating CME region, are spread in *cis* across *FLC* to mediate the formation of a Polycomb-repressed domain at *FLC* after cold. EBS and SHL interact with themselves and each other to form a multimeric assembly along *FLC* chromatin, which conceptually promotes these proteins to reach neighboring nucleosomes. In support of the *cis*-spreading mode, a functional loss of VAL1 that recognizes only the *cis*-acting CME results in a strong reduction of EBS in the CME region and at the spreading sites.

Several lncRNAs from the *FLC* locus have been previously described to induce or mediate Polycomb repression of *FLC* in response to prolonged cold (reviewed in Costa and Dean[36]). Our results show that the bivalent CME confers cold-induced Polycomb repression at the recombinant *GUS* fusion gene that lacks any sequence from *FLC* except for the 47-bp CME. This provides compelling evidence that it is the *cis*-acting CME together with its bivalency feature to drive cold-induced switching of the highly activated *FLC* chromatin state to a Polycomb-repressed state and thus to confer Polycomb silencing at *FLC* by vernalization.

We have previously reported that LHP1 (reading H3K27me3, but not H3K4me3) is involved in the establishment of the H3K27me3 peak in the CME region in cold and maintenance of stable *FLC* silencing in the warm.[5] Intriguingly, it was reported that LHP1 is not involved in the H3K27me3 nucleation in cold, but only mediates H3K27me3 spreading across *FLC* in the warm.[3] We confirmed that *LHP1* indeed is required for both H3K27me3 nucleation (in cold) and spreading (in warmth) (Figure S7F). It appears that LHP1 alone only plays a moderate

role in cold-induced Polycomb repression at *FLC* because the loss of *LHP1* function causes only a moderate reactivation of *FLC* expression in warmth.[3] In contrast, the functional loss of *EBS* together with *SHL* results in a near elimination of H3K27me3 spreading and full reactivation of *FLC* expression after return to warmth, revealing that their essential role in PcG-mediated *FLC* repression by vernalization. The triple mutant *lhp1 ebs shl* is not viable,[25] which prevents us from analyzing functional redundancy among these readers. A future study would be required to determine how LHP1 may function together with EBS and SHL to mediate cold-induced H3K27me3 nucleation and subsequent spreading at *FLC*.

The CME chromatin at *FLC* is in the bivalent state before, during, and post cold exposure. Throughout the life cycle, the *FLC* chromatin state in *Arabidopsis* is dynamically regulated in response to developmental and environmental signals.[2,42] Before cold, the high level of H3K4me3 in the bivalent CME region promotes *FLC* expression to prevent the floral transition[7,17]; in cold-induced chromatin-state switching, the pre-existing H3K27me3 marks in the bivalent CME region can promote initial H3K27 trimethylation by VIN3-PRC2 in cold because the binding of PRC2 to pre-existing H3K27me3 marks is known to cause an allosteric activation of its methylation activity.[43,44] During post-cold growth in warmth, the Polycomb-repressed state at *FLC* (with a bivalent CME region) is maintained through cell divisions. In subsequent reproduction, the H3K27me3 marks at *FLC* are erased in sperm cells by a genome-wide reprogramming mechanism,[45] and the cold-induced Polycomb-repressed state at *FLC* is transmitted to the zygote through the egg cell.[46] It is likely that the bivalency in the CME region may be transmitted to the zygote through the egg cell to mediate dynamic *FLC* regulation in next generation.

H3K4me3 is a common histone mark for actively transcribed genes in eukaryotes and often functions to promote gene expression.[33,34] We have found that the bivalent chromatin readers EBS and SHL read the H3K4me3 marks in a bivalent regulatory region through their PHD domains and directly interact with Polycomb factors to switch an active chromatin state to Polycomb-repressed in response to an environmental stimulus. These findings define a paradigm for switching an active chromatin state at the loci with bivalent regulatory regions to Polycomb-repressed state in response to environmental signals.

Limitations of the study

We focused on cold-induced switching of the chromatin state at *FLC*. In addition to the CME region, there are various bivalent regions in the *Arabidopsis* genome, and sequencing and further analyzing of DNA fragments from K4-K27 and K27-K4 re-ChIP will be a critical next step to identify and characterize the features of genome-wide bivalent regions. In addition, it would be interesting to explore whether and how other bivalent regulatory regions, like CME, function together with EBS and/or SHL to mediate chromatin-state switching in response to environmental and/or developmental signals in land plants.

STAR★METHODS

Detailed methods are provided in the online version of this paper and include the following:

SUPPLEMENTAL INFORMATION

Supplemental information can be found online at https://doi.org/10.1016/j.molcel.2023.02.014.

ACKNOWLEDGMENTS

We thank for Drs. Zicong Li and De Niu for experimental assistance and Dr. Peng Li for bioinformatic analysis. This work was supported in part by the National Natural Science Foundation of China (grant nos. 31830049 and 31721001 to Y.H.), the Peking-Tsinghua Center for Life Sciences, and the Chinese Academy of Sciences (XDB27030202 to Y.H.).

AUTHOR CONTRIBUTIONS

Y.H. conceived and supervised the research. Z.G. and Y.L. designed and performed most of the experiments. Y.O., M.Y., T.C., and R.L. performed part of the experiments. Z.G., Y.L., Y.H., Y.O., M.Y., T.C., and X.Z. analyzed the data. Y.H. and Y.L. wrote the paper with the help from Z.G.

DECLARATION OF INTERESTS

The authors declare no competing interests.

INCLUSION AND DIVERSITY

We support inclusive, diverse, and equitable conduct of research.

Received: June 7, 2022
Revised: December 27, 2022
Accepted: February 14, 2023
Published: March 14, 2023

REFERENCES

1. Blackledge, N.P., and Klose, R.J. (2021). The molecular principles of gene regulation by Polycomb repressive complexes. Nat. Rev. Mol. Cell Biol. *22*, 815–833.
2. Bouché, F., Woods, D.P., and Amasino, R.M. (2017). Winter memory throughout the plant kingdom: different paths to flowering. Plant Physiol. *173*, 27–35.
3. Yang, H., Berry, S., Olsson, T.S.G., Hartley, M., Howard, M., and Dean, C. (2017). Distinct phases of Polycomb silencing to hold epigenetic memory of cold in Arabidopsis. Science *357*, 1142–1145.

4. Andrés, F., and Coupland, G. (2012). The genetic basis of flowering responses to seasonal cues. Nat. Rev. Genet. *13*, 627–639.
5. Yuan, W., Luo, X., Li, Z., Yang, W., Wang, Y., Liu, R., Du, J., and He, Y. (2016). A *cis* cold memory element and a *trans* epigenome reader mediate Polycomb silencing of *FLC* by vernalization in Arabidopsis. Nat. Genet. *48*, 1527–1534.
6. Choi, K., Kim, J., Hwang, H.J., Kim, S., Park, C., Kim, S.Y., and Lee, I. (2011). The FRIGIDA complex activates transcription of *FLC*, a strong flowering repressor in Arabidopsis, by recruiting chromatin modification factors. Plant Cell *23*, 289–303.
7. Li, Z., Jiang, D., and He, Y. (2018). FRIGIDA establishes a local chromosomal environment for *FLOWERING LOCUS C* mRNA production. Nat. Plants *4*, 836–846.
8. Zhu, P., Lister, C., and Dean, C. (2021). Cold-induced Arabidopsis FRIGIDA nuclear condensates for *FLC* repression. Nature *599*, 657–661.
9. Sung, S., and Amasino, R.M. (2004). Vernalization in *Arabidopsis thaliana* is mediated by the PhD finger protein VIN3. Nature *427*, 159–164.
10. Heo, J.B., and Sung, S. (2011). Vernalization-mediated epigenetic silencing by a long intronic noncoding RNA. Science *331*, 76–79.
11. Wood, C.C., Robertson, M., Tanner, G., Peacock, W.J., Dennis, E.S., and Helliwell, C.A. (2006). The *Arabidopsis thaliana* vernalization response requires a Polycomb-like protein complex that also includes VERNALIZATION INSENSITIVE 3. Proc. Natl. Acad. Sci. USA *103*, 14631–14636.
12. Angel, A., Song, J., Dean, C., and Howard, M. (2011). A Polycomb-based switch underlying quantitative epigenetic memory. Nature *476*, 105–108.
13. Qüesta, J.I., Song, J., Geraldo, N., An, H., and Dean, C. (2016). Arabidopsis transcriptional repressor *VAL1* triggers Polycomb silencing at *FLC* during vernalization. Science *353*, 485–488.
14. Finnegan, E.J., and Dennis, E.S. (2007). Vernalization-induced trimethylation of histone H3 lysine 27 at *FLC* is not maintained in mitotically quiescent cells. Curr. Biol. *17*, 1978–1983.
15. Sung, S., and Amasino, R.M. (2004). Vernalization and epigenetics: how plants remember winter. Curr. Opin. Plant Biol. *7*, 4–10.
16. Jiang, D., and Berger, F. (2017). DNA replication-coupled histone modification maintains Polycomb gene silencing in plants. Science *357*, 1146–1149.
17. Jiang, D., Gu, X., and He, Y. (2009). Establishment of the winter-annual growth habit via FRIGIDA-mediated histone methylation at *FLOWERING LOCUS C* in Arabidopsis. Plant Cell *21*, 1733–1746.
18. Yang, H., Howard, M., and Dean, C. (2014). Antagonistic roles for H3K36me3 and H3K27me3 in the cold-induced epigenetic switch at Arabidopsis *FLC*. Curr. Biol. *24*, 1793–1797.
19. Bernstein, B.E., Mikkelsen, T.S., Xie, X., Kamal, M., Huebert, D.J., Cuff, J., Fry, B., Meissner, A., Wernig, M., Plath, K., et al. (2006). A bivalent chromatin structure marks key developmental genes in embryonic stem cells. Cell *125*, 315–326.
20. Voigt, P., LeRoy, G., Drury, W.J., Zee, B.M., Son, J., Beck, D.B., Young, N.L., Garcia, B.A., and Reinberg, D. (2012). Asymmetrically modified nucleosomes. Cell *151*, 181–193.
21. Zhang, J., Zhang, Y., You, Q., Huang, C., Zhang, T.T., Wang, M., Zhang, T.W., Yang, X., Xiong, J., Li, Y., et al. (2022). Highly enriched BEND3 prevents the premature activation of bivalent genes during differentiation. Science *375*, 1053–1058.
22. Zhang, X., Bernatavichute, Y.V., Cokus, S., Pellegrini, M., and Jacobsen, S.E. (2009). Genome-wide analysis of mono-, di- and trimethylation of histone H3 lysine 4 in Arabidopsis thaliana. Genome Biol. *10*, R62.
23. Zhang, J.X., Xie, S.J., Cheng, J.K., Lai, J.S., Zhu, J.K., and Gong, Z.Z. (2016). The second subunit of DNA polymerase Delta is required for genomic stability and epigenetic regulation. Plant Physiol. *171*, 1192–1208.
24. Patel, D.J., and Wang, Z.X. (2013). Readout of epigenetic modifications. Annu. Rev. Biochem. *82*, 81–118.
25. Li, Z., Fu, X., Wang, Y., Liu, R., and He, Y. (2018). Polycomb-mediated gene silencing by the BAH-EMF1 complex in plants. Nat. Genet. *50*, 1254–1261.
26. Qian, S., Lv, X., Scheid, R.N., Lu, L., Yang, Z., Chen, W., Liu, R., Boersma, M.D., Denu, J.M., Zhong, X., and Du, J. (2018). Dual recognition of H3K4me3 and H3K27me3 by a plant histone reader SHL. Nat. Commun. *9*, 2425.
27. Yang, Z., Qian, S., Scheid, R.N., Lu, L., Chen, X., Liu, R., Du, X., Lv, X., Boersma, M.D., Scalf, M., et al. (2018). EBS is a bivalent histone reader that regulates floral phase transition in Arabidopsis. Nat. Genet. *50*, 1247–1253.
28. López-González, L., Mouriz, A., Narro-Diego, L., Bustos, R., Martínez-Zapater, J.M., Jarillo, J.A., and Piñeiro, M. (2014). Chromatin-dependent repression of the Arabidopsis floral integrator genes involves plant specific PhD-containing proteins. Plant Cell *26*, 3922–3938.
29. Lee, I., Michaels, S.D., Masshardt, A.S., and Amasino, R.M. (1994). The late-flowering phenotype of *FRIGIDA* and *luminidependens* is suppressed in the Landsberg *erecta* strain of *Arabidopsis*. Plant J. *6*, 903–909.
30. Oksuz, O., Narendra, V., Lee, C.H., Descostes, N., LeRoy, G., Raviram, R., Blumenberg, L., Karch, K., Rocha, P.P., Garcia, B.A., et al. (2018). Capturing the onset of PRC2-mediated repressive domain formation. Mol. Cell *70*, 1149–1162.e5.
31. Greb, T., Mylne, J.S., Crevillen, P., Geraldo, N., An, H., Gendall, A.R., and Dean, C. (2007). The PhD finger protein VRN5 functions in the epigenetic silencing of Arabidopsis FLC. Curr. Biol. *17*, 73–78.
32. Sung, S., Schmitz, R.J., and Amasino, R.M. (2006). A PHD finger protein involved in both the vernalization and photoperiod pathways in Arabidopsis. Genes Dev. *20*, 3244–3248.
33. Shilatifard, A. (2012). The COMPASS family of histone H3K4 methylases: mechanisms of regulation in development and disease pathogenesis. Annu. Rev. Biochem. *81*, 65–95.
34. Voigt, P., Tee, W.W., and Reinberg, D. (2013). A double take on bivalent promoters. Genes Dev. *27*, 1318–1338.
35. Narusaka, Y., Nakashima, K., Shinwari, Z.K., Sakuma, Y., Furihata, T., Abe, H., Narusaka, M., Shinozaki, K., and Yamaguchi-Shinozaki, K. (2003). Interaction between two cis-acting elements, ABRE and DRE, in ABA-dependent expression of Arabidopsis rd29A gene in response to dehydration and high-salinity stresses. Plant J. *34*, 137–148.
36. Costa, S., and Dean, C. (2019). Storing memories: the distinct phases of Polycomb-mediated silencing of Arabidopsis *FLC*. Biochem. Soc. Trans. *47*, 1187–1196.
37. Grau, D., Zhang, Y.X., Lee, C.H., Valencia-Sánchez, M., Zhang, J., Wang, M., Holder, M., Svetlov, V., Tan, D.Y., Nudler, E., et al. (2021). Structures of monomeric and dimeric PRC2:EZH1 reveal flexible modules involved in chromatin compaction. Nat. Commun. *12*, 714.
38. Laprell, F., Finkl, K., and Müller, J. (2017). Propagation of Polycomb-repressed chromatin requires sequence-specific recruitment to DNA. Science *356*, 85–88.
39. Coleman, R.T., and Struhl, G. (2017). Causal role for inheritance of H3K27me3 in maintaining the OFF state of a *Drosophila HOX* gene. Science *356*, eaai8236.
40. Wang, X., and Moazed, D. (2017). DNA sequence-dependent epigenetic inheritance of gene silencing and histone H3K9 methylation. Science *356*, 88–91.
41. Wang, X., Paulo, J.A., Li, X., Zhou, H., Yu, J., Gygi, S.P., and Moazed, D. (2021). A composite DNA element that functions as a maintainer required for epigenetic inheritance of heterochromatin. Mol. Cell *81*, 3979–3991.e4.
42. Gao, Z., Zhou, Y., and He, Y. (2022). Molecular epigenetic mechanisms for the memory of temperature stresses in plants. J. Genet. Genomics *49*, 991–1001.
43. Margueron, R., Justin, N., Ohno, K., Sharpe, M.L., Son, J., Drury, W.J., Voigt, P., Martin, S.R., Taylor, W.R., De Marco, V., et al. (2009). Role of

the polycomb protein EED in the propagation of repressive histone marks. Nature *461*, 762–767.

44. Xu, C., Bian, C.B., Yang, W., Galka, M., Ouyang, H., Chen, C., Qiu, W., Liu, H.D., Jones, A.E., MacKenzie, F., et al. (2010). Binding of different histone marks differentially regulates the activity and specificity of Polycomb repressive complex 2 (PRC2). Proc. Natl. Acad. Sci. USA *107*, 19266–19271.
45. Borg, M., Jacob, Y., Susaki, D., LeBlanc, C., Buendía, D., Axelsson, E., Kawashima, T., Voigt, P., Boavida, L., Becker, J., et al. (2020). Targeted reprogramming of H3K27me3 resets epigenetic memory in plant paternal chromatin. Nat. Cell Biol. *22*, 621–629.
46. Luo, X., Ou, Y., Li, R.J., and He, Y.H. (2020). Maternal transmission of the epigenetic 'memory of winter cold' in Arabidopsis. Nat. Plants *6*, 1211–1218.
47. Suzuki, M., Wang, H.H., and McCarty, D.R. (2007). Repression of the *LEAFY COTYLEDON 1/B3* regulatory network in plant embryo development by *VP1/ABSCISIC ACID INSENSITIVE 3-LIKE B3* genes. Plant Physiol *143*, 902–911.
48. Karimi, M., De Meyer, B., and Hilson, P. (2005). Modular cloning in plant cells. Trends Plant Sci. *10*, 103–105.
49. Schwab, R., Ossowski, S., Riester, M., Warthmann, N., and Weigel, D. (2006). Highly specific gene silencing by artificial microRNAs in Arabidopsis. Plant Cell *18*, 1121–1133.
50. Zuo, J., Niu, Q.W., and Chua, N.H. (2000). Technical advance: an estrogen receptor-based transactivator XVE mediates highly inducible gene expression in transgenic plants. Plant J. *24*, 265–273.
51. Lu, Q., Tang, X., Tian, G., Wang, F., Liu, K., Nguyen, V., Kohalmi, S.E., Keller, W.A., Tsang, E.W., Harada, J.J., et al. (2010). Arabidopsis homolog of the yeast TREX-2 mRNA export complex: components and anchoring nucleoporin. Plant J. *61*, 259–270.
52. Gu, X., Le, C., Wang, Y., Li, Z., Jiang, D., Wang, Y., and He, Y. (2013). Arabidopsis FLC clade members form flowering-repressor complexes coordinating responses to endogenous and environmental cues. Nat. Commun. *4*, 1947.
53. Jiang, D., Kong, N.C., Gu, X., Li, Z., and He, Y. (2011). Arabidopsis COMPASS-like complexes mediate histone H3 lysine-4 trimethylation to control floral transition and plant development. PLoS Genet. *7*, e1001330.
54. Wang, Y., Gu, X., Yuan, W., Schmitz, R.J., and He, Y. (2014). Photoperiodic control of the floral transition through a distinct Polycomb repressive complex. Dev. Cell *28*, 727–736.
55. Desvoyes, B., Sequeira-Mendes, J., Vergara, Z., Madeira, S., and Gutierrez, C. (2018). Sequential ChIP protocol for profiling bivalent epigenetic modifications (ReChIP). Methods Mol. Biol. *1675*, 83–97.
56. Wysocka, J., Swigut, T., Milne, T.A., Dou, Y.L., Zhang, X., Burlingame, A.L., Roeder, R.G., Brivanlou, A.H., and Allis, C.D. (2005). WDR5 associates with histone H3 methylated at K4 and is essential for H3K4 methylation and vertebrate development. Cell *121*, 859–872.
57. Tao, Z., Shen, L., Gu, X., Wang, Y., Yu, H., and He, Y. (2017). Embryonic epigenetic reprogramming by a pioneer transcription factor in plants. Nature *551*, 124–128.

Please cite this article in press as: Gao et al., A pair of readers of bivalent chromatin mediate formation of Polycomb-based "memory of cold" in plants, Molecular Cell (2023), https://doi.org/10.1016/j.molcel.2023.02.014

CellPress

STAR★METHODS

KEY RESOURCES TABLE

REAGENT or RESOURCE	SOURCE	IDENTIFIER
Antibodies		
Monoclonal ANTI-FLAG® M2-Peroxidase (HRP) antibody produced in mouse)	Sigma-Aldrich	Cat# A8592; RRID: AB_439702
Anti-HA High Affinity	Roche	Cat# 11867423001; RRID: AB_390918
ANTI-FLAG® antibody produced in rabbit	Sigma-Aldrich	Cat# F7425; RRID: AB_439687
Anti-HA antibody produced in rabbit	Sigma-Aldrich	Cat# H6908; RRID: AB_260070
anti-H3K27me3 antibody	Millipore	Cat# 07-449; RRID: AB_310624
anti-H3K4me2 antibody	Millipore	Cat# 07-030; RRID: AB_310342
anti-H3K4me3 antibody	Millipore	Cat# 05-745R; RRID: AB_1587134
anti-GST antibody	Sigma-Aldrich	Cat# G7781; RRID: AB_259965
anti-VIN3 antibody	ABclonal Technology	N/A
Bacterial and virus strains		
Escherichia coli (E. coli) DH5α competent cell	Lab stock	N/A
E. coli BL21 (DE3) competent cell	Lab stock	N/A
Agrobacterium tumefaciens GV3101 competent cell	Lab stock	N/A
Chemicals, peptides, and recombinant proteins		
β-Estradiol	Sigma-Aldrich	Cat# E8875
5-bromo-4-chloro-3-indolyl-β-D-glucuronic acid (X-Gluc)	Thermo Scientific	Cat# R0851
Trimethyl-Histone H3 (Lys27) peptide, biotin conjugate	Sigma-Aldrich	Cat# 12-565
Avidin-Agarose	Sigma-Aldrich	Cat# A9207
EZview™ Red ANTI-FLAG® M2 Affinity Gel	Sigma-Aldrich	Cat# F2426
Pierce™ Anti-HA Magnetic Beads	Thermo Scientific	Cat# 88836
Anti-FLAG® M2 Magnetic Beads	Sigma-Aldrich	Cat# M8823
Protease inhibitor cocktail	Roche	Cat# 04693132001
Critical commercial assays		
NEBNext® Ultra™ II DNA Library Prep Kit for Illumina®	New England Biolabs	Cat# E7645S
Eastep® Super Total RNA Extraction Kit	Promega	Cat# LS1040
HiScript III 1st Strand cDNA Synthesis Kit (+gDNA wiper)	Vazyme	Cat# R312-01
Magna ChIP™ A/G Chromatin Immunoprecipitation Kit	Merck	Cat# 17-10085
pEASY®-Uni Seamless Cloning and Assembly Kit	TransGen Biotech	Cat# CU101-01
Deposited data		
H3K4me3 ChIP-seq raw data	https://www.ncbi.nlm.nih.gov/geo/	GSE185121
H3K27me3 ChIP-seq raw data	https://www.ncbi.nlm.nih.gov/geo/	GSE185120
Experimental models: Organisms/strains		
Arabidopsis: Col-0	Lab stock	N/A
Arabidopsis: Col-*FRI*	Lee et al.[29]	N/A
Arabidopsis: *shl*	Li et al.[7]	N/A
Arabidopsis: *FRI shl*	This paper	N/A

(*Continued on next page*)

Please cite this article in press as: Gao et al., A pair of readers of bivalent chromatin mediate formation of Polycomb-based "memory of cold" in plants, Molecular Cell (2023), https://doi.org/10.1016/j.molcel.2023.02.014

Continued

REAGENT or RESOURCE	SOURCE	IDENTIFIER
Arabidopsis: ebs	Li et al.[7]	CS906904
Arabidopsis: FRI ebs	This paper	N/A
Arabidopsis: FRI ebs shl	This paper	N/A
Arabidopsis: val2	Suzuki et al.[47]	N/A
Arabidopsis: FRI val2	This paper	N/A
Arabidopsis: EBS.1-Flag	Li et al.[7]	N/A
Arabidopsis: EBS.2-Flag	Li et al.[7]	N/A
Arabidopsis: SHL:HA	Li et al.[7]	
Arabidopsis: HA:SHL	This paper	N/A
Arabidopsis: VAL1:Flag	Yuan et al.[5]	N/A
Arabidopsis: FRI vin3	Sung and Amasino[9]	N/A
Saccharomyces. cerevisiae AH109	Clontech	Cat# PT3247-1
Oligonucleotides		
Primers used in this study are listed in Table S1	N/A	N/A
Recombinant DNA		
Plasmid: *EBS:FLAG*	Li et al.[7,25]	N/A
Plasmid: *HA:SHL*	This paper	N/A
Plasmid: *EBS(P41L):FLAG*	This paper	N/A
Plasmid: *EBS(Y155A):FLAG*	This paper	N/A
Plasmid: *HA:SHL(W63L/Y65A)*	This paper	N/A
Plasmid: *HA:SHL(F141A/Y148A)*	This paper	N/A
Plasmid: *AD/BD-EBS*	This paper	N/A
Plasmid: *AD/BD-BAH$_{EBS}$*	This paper	N/A
Plasmid: *AD/BD-PHD$_{EBS}$*	This paper	N/A
Plasmid: *AD/BD-SHL*	This paper	N/A
Plasmid: *AD/BD-BAH$_{SHL}$*	This paper	N/A
Plasmid: *AD/BD-PHD$_{SHL}$*	This paper	N/A
Plasmid: *AD-VID$_{VIN3}$*	This paper	N/A
Plasmid: *AD-VID$_{VRN5}$*	This paper	N/A
Plasmid: *pER8-VAL1-amiRNA*	This paper	N/A
Plasmid: *CME-GUS*	Yuan et al.[5]	N/A
Plasmid: *pCOR78-VIN3*	This paper	N/A
Software and algorithms		
GraphPad Prism	N/A	https://www.graphpad-prism.cn/
Microsoft Excel	Microsoft	N/A

RESOURCE AVAILABILITY

Lead contact

Further inquiries and requests for materials should be directed to the lead contact, Yuehui He (yhhe@pku.edu.cn).

Materials availability

Transgenic lines and plasmids generated in this study are described in the key resources table and available upon requests made to the lead contact.

Data and code availability

- The ChIP-seq data listed in the key resources table are available on NCBI's Gene Expression Omnibus database with the following accession numbers (GSE185120 and GSE185121).
- This paper does not report original code.
- Any additional information required to reanalyze the data reported in this paper is available from the lead contact upon request.

EXPERIMENTAL MODEL AND SUBJECT DETAILS

Arabidopsis thaliana strains were used in this study. Seeds were sterilized and germinated on half-strength MS medium. Col-0, Col-*FRI*, *shl*, *ebs*, *ebs shl*, *val1*, *val2*, *FRI vin3*, and the transgenic lines including *EBS.1-Flag/ebs shl*, *EBS.2-Flag (EBS:Flag)/ebs shl* and *SHL:HA/ebs shl* have been described previously.[5,9,25,29] Plants were grown under cool white light in long days (16-h light /8-h dark) at around 22°C.

For prolonged cold treatments, seeds were germinated on half-strength MS medium and grown for about 5 days at 22°C, and subsequently, the seedlings were transferred to a 4°C short-day growth chamber (8-h light /16-h dark) for 2 to 6 weeks, followed by return to the normal growth condition (long days at around 22°C).

Nicotiana benthamiana plants were grown under cool white light in long days (16-h light /8-h dark) at around 25°C.

METHOD DETAILS

Plasmid constructions

To generate *EBS:HA* or *EBS:Flag* plasmid, a 3.9-kb genomic sequence of *EBS* (1.8-kb promoter plus 2.1-kb genomic coding region without stop codon) was fused in frame with three copies of *HA* (or *Flag*) (at the C terminus) at a modified *pENTR3C* vector (Invitrogen) through *BamHI* and *XhoI*, and the gene fusion was subsequently recombined into the binary vector *pHGW*,[48] through Gateway technology (Invitrogen). To create *HA:SHL*, a 4.6-kb genomic sequence of *SHL* (2.1-kb promoter, 1.8-kb genomic coding region and 0.7-kb terminator) with one copy of *HA* inserted at the N-terminus, was cloned into *pHGW*.[48] *EBS:Flag* and *HA:SHL* transgenes with point mutations including P41L, Y155A, W63L/Y65A and F141A/Y148A, were created by overlapping PCR. Primers are listed in Table S1.

To construct the plasmids for yeast two-hybrid assays, the full-length coding sequence (CDS) of *EBS*, BAH_{EBS} (for amino acids/aa 29 to 144) and PHD_{EBS} (for aa 146 to 197) were cloned into *pGADT7* (AD) and/or *pGBKT7* (BD) (Clontech) at *EcoRI* and *BamHI*. Similarly, *AD/BD-SHL* (full-length CDS), *AD/BD-*BAH_{SHL} (for aa 21 to 137) and *AD/BD-*PHD_{SHL} (for aa139 to 190) were constructed. *AD-*VID_{VIN3} (for aa 512 to 620) was cloned into *pGADT7* at *NcoI* and *XmaI*, and *AD-*VID_{VRN5} (for aa 502 to 602) was cloned into *pGADT7* at *NdeI* and *EcoRI*.

To generate the inducible *VAL1* knock-down construct *pER8-VAL1-amiRNA*, a DNA fragment encoding an artificial microRNA targeting *VAL1* (5'-TGTATGCATGGAGTCACACCT-3') was cloned into *pRS300*,[49] and subsequently, the amiRNA-production cassette was cloned into the *pER8* vector downstream of a β-estradiol inducible promoter.[50] To construct *pCOR78-VIN3*, a 0.7-kb *COR78* promotor region fused with the 2.1-kb coding sequence for VIN3, was cloned into *pCAMBIA1300* by seamless cloning (TransGen Biotech). The CDS of *SHL* (minus the stop codon) was fused in frame with the CDS for an N-terminal YFP fragment in *pEarleyagte201-YN* and the CDS for a C-terminal YFP fragment in *pEarleygate202-YC*,[51] resulting in *SHL-nYFP* and *SHL-cYFP*, respectively.

mRNA expression analysis

Total RNAs were extracted from aerial parts of non-vernalized or vernalized seedlings with Eastep Super Total RNA extraction kit (Promega, LS1040) according to the manufacturer's instructions. Following reverse transcription, real-time quantitative PCR (qPCR) was conducted on an ABI *QuantStudio6 Flex* real-time PCR system using a SYBR Green master mix (Yeasen, 11201ES03), as previously described.[52] Three biological replicates were performed, and each sample was quantified in triplicate and normalized to the constitutively-expressed endogenous reference gene *PROTEIN PHOSPHATASE 2A* (*PP2A*).[10] The primers for *FLC*, *FT*, *VAL1*, *TUB2* and *PP2A* amplifications are listed in Table S1.

For quantification of unspliced *CME:GUS* transcripts, residual genomic DNA was removed, followed by reverse transcription using HiScript III 1st Strand cDNA Synthesis Kit (+gDNA wiper) according to the manufacturer's instructions (Vazyme, R312-01). Subsequently, qPCR was performed to measure the unspliced transcripts of *CME:GUS* and *PP2A* (endogenous control). Primer sequences are specified in Table S1.

Yeast two-hybrid assay (Y2H)

Y2H experiments were carried out with Matchmarker GAL4 Two-Hybrid System (Clontech) following the manufacturer's protocols. BAH_{EBS} (aa 29 to 144), PHD_{EBS} (aa 146 to 197), BAH_{SHL} (aa 21 to 137), PHD_{SHL} (aa 139 to 190), VID_{VIN3} (aa 512 to 620) and VID_{VRN5} (aa 502 to 602) were fused with the GAL4-AD or BD domain. The yeast cells of *AH109* were co-transformed with paired plasmids, and subsequently spread on a highly-stringent synthetic defined (SD) growth medium without adenine (A), histidine (H), leucine (L) and tryptophan (W) or a growth control medium without leucine and tryptophan, SD (-WL).

Bimolecular fluorescence complementation (BiFC)

BiFC assays were carried out with a split-YFP system in *Nicotiana benthamiana* leaves, as previously described with minor modifications.[51] Briefly, the *Agrobacterium* GV3101 cells harboring *SHL-nYFP* or *SHL-cYFP* were cultured overnight, and re-suspended in an infiltration buffer. Equal volumes of each culture were mixed and then infiltrated into tobacco leaves. YFP fluorescence in the epidermal cells was observed 2-3 days after infiltration by an LSM900 laser scanning confocal microscopy (ZEISS). Nuclei were stained by a DAPI (4',6-diamidino-2-phenylindole) solution (0.1 μg/ml) shortly before fluorescence observation.

Please cite this article in press as: Gao et al., A pair of readers of bivalent chromatin mediate formation of Polycomb-based "memory of cold" in plants, Molecular Cell (2023), https://doi.org/10.1016/j.molcel.2023.02.014

Co-immunoprecipitation (Co-IP)

Co-IP experiments were performed as previously described with minor variations.[53] Briefly, total proteins were extracted from around 0.5-g seedlings (cold-treated or untreated) expressing the proteins of interest, followed by immunoprecipitations with anti-Flag M2 affinity gel (Sigma, F2426) or anti-HA magnetic beads (Thermo Scientific, 88836). VAL1:Flag, EBS:HA or SHL:HA in the immunoprecipitates were detected by western blotting with anti-Flag (Sigma, A8592) or anti-HA (Roche, 11867423001).

For co-immunoprecipitation of EBS with VIN3, wild-type seedlings (Col-*FRI*) or seedlings expressing EBS:Flag were cold-treated for 4 weeks. Subsequently, total proteins were extracted from the vernalized seedlings and immunoprecipitated with anti-Flag M2 magnetic beads (Sigma, M8823), followed by western blotting with rabbit polyclonal anti-VIN3 (produced by ABclonal Technology, China).

Chromatin immunoprecipitation (ChIP)

ChIP assays were performed with the Magna ChIP kit (Merck, 17-10085) as previously described with minor variations.[54] In brief, around 0.4-g vernalized or non-vernalized seedlings were harvested, followed by total chromatin extraction. After chromatin sonication, immunoprecipitations were carried out with anti-Flag (Sigma, F7425), anti-HA (Sigma, H6908), anti-H3K27me3 (Millipore, 07-449) or anti-H3K4me2 (Millipore, 07-030). qPCR was conducted on an ABI *QuantStudio6 Flex* real-time PCR system, to quantify the levels of immunoprecipitated genomic fragments of interest. Biological replicates were carried out and each sample was quantified in triplicate. Primers are listed in Table S1.

Sequential chromatin immunoprecipitation (reChIP)

Sequential chromatin immunoprecipitations were conducted following a previously described protocol with minor modifications.[55] Briefly, around 1.0 g of non-vernalized or vernalized (28-d cold-treated) seedlings were harvested for total chromatin extraction; subsequently, chromatin was fragmentized by a UCD-200 sonicator (Diagenode) with 16 cycles of sonication at the high-power mode (30 second ON and 30 second OFF), resulting in fragments of about 150-500 bp with major bands around 250 bp. The first immunoprecipitation was performed with anti-H3K4me3 (Millipore, 05-745R) or anti-H3K27me3 (Millipore, 07-449); subsequently, the immunoprecipitated chromatin fragments were eluted with an elution buffer (50 mM Tris-HCl /pH 8, 5 mM EDTA, 20 mM DTT and 1% SDS). After removal of SDS and DTT, the cleaned chromatin fragments were subjected to another round of immunoprecipitations with anti-H3K4me3 or anti-H3K27me3 (IgG as negative control). qPCR was conducted to measure the levels of immunoprecipitated genomic fragments of interest. Three biological replicates were performed in parallel. Primers are listed in Table S1.

Histone 3 peptide pulldown

Pulldown assays were conducted as previously described with minor modifications.[56] Briefly, 1.0 μg of each H3 peptide with trimethylated K4 (Sigma, 12-564) or trimethylated K27 conjugated to biotin (Sigma, 12-565) was incubated with 10 μl of avidin agarose (Sigma, A9207), followed by precleaning with the binding buffer (50 mM Tris–HCl pH 7.5, 100 mM NaCl, 0.2% glycerol and 1x protease inhibitor cocktail). Purified GST-EBS, GST-EBS$_{P41L}$ and GST-EBS$_{Y155A}$ proteins were firstly precleared by incubating with avidin agarose beads and subsequently were incubated with H3 peptide-bound beads, followed by precipitation and washing (three times). GST-fused proteins were eluted from the precipitated beads and analyzed by western blotting using anti-GST (Sigma, G7781).

β-Estradiol application

β-estradiol (Sigma, E8875) was dissolved in ethanol to make a 20 mM stock. Subsequently, 60 μM of β-estradiol or mock (0.3% ethanol) was applied to the cold-treated *FRI val2* seedlings expressing a β-estradiol-inducible *VAL1* knockdown cassette (*pER8-VAL1-amiRNA*), starting from Day 33 in cold until flowering (note that seedings were exposed to cold for 35 d and returned to warmth subsequently). Chemical applications were conducted daily.

Histochemical β-glucuronidase (GUS) staining

Seedlings were stained at 37°C for 22 h in a solution of 5 mM EDTA pH 8.0, 0.05% Triton X-100, 2 mM potassium ferrocyanide, 2 mM potassium ferricyanide, 100 mM NaH_2PO_4, 100 mM Na_2HPO_4, and 0.5 mg/ml 5-bromo-4-chloro-3-indolyl-β-D-glucuronic acid (X-Gluc), followed by chlorophyll removal in 70% ethanol, as described previously.[57]

QUANTIFICATION AND STATISTICAL ANALYSIS

Two-tailed Student's *t* test was performed using *Excel*, and one-way analysis of variance (ANOVA) was conducted with Holm-Sidak method using *GraphPad Prism* (v9.1.1).

Molecular Cell, Volume *83*

Supplemental information

A pair of readers of bivalent chromatin mediate formation of Polycomb-based “memory of cold” in plants

Zheng Gao, Yaxiao Li, Yang Ou, Mengnan Yin, Tao Chen, Xiaolin Zeng, Renjie Li, and Yuehui He

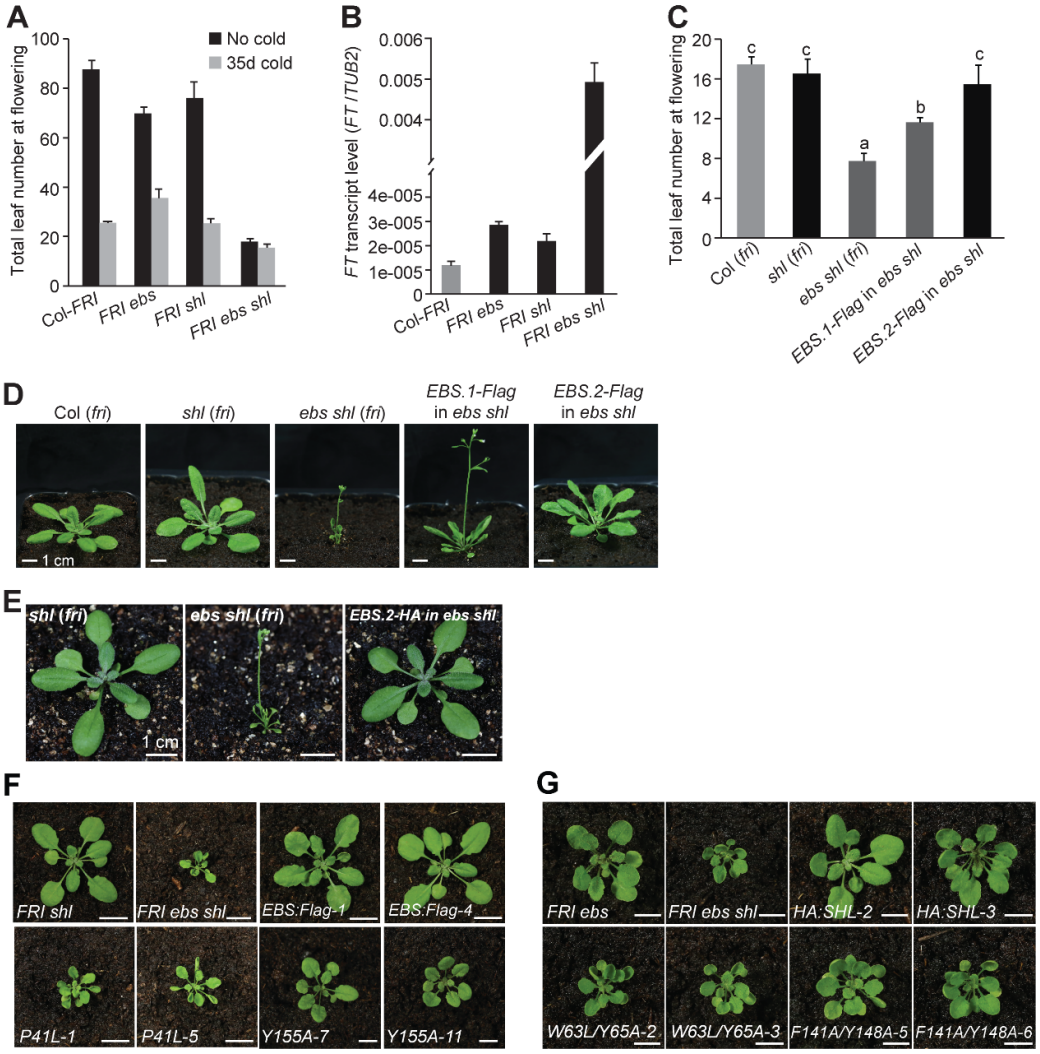

Figure S1. Characterization of the *FRI ebs*, *FRI shl* and *FRI ebs shl* mutants and functional analysis of Flag- or HA-tagged EBS and SHL, related to Figures 1 and 3. (A) Total number of leaves formed prior to flowering of the indicated lines grown in long days. No cold, non-vernalized; 35d cold, cold-treated or vernalized for 35 days. 19-26 plants per line were scored; error bars for s.d. (B) *FT* transcript levels in the indicated seedlings grown under normal temperature. Data were normalized to the constitutively expressed *TUBULIN2* (*TUB2*); error bars for s.d. of three biological replicates. (C) *EBS.2-Flag*, but not *EBS.1-Flag*, fully rescued the early flowering in *ebs shl*. *ebs shl* is in a Col background, with a mutant *fri* allele.[S1] The total number of leaves formed prior to flowering in 12-16 plants per line was scored; error bars for s.d. Letters indicate statistically-significant differences (one-way ANOVA, $p<0.05$). (D) Phenotypes of the late-stage *EBS.1-Flag* and *EBS.2-Flag* plants grown in long days. (E) *EBS.2-HA* is fully functional. (F) Phenotypes of *EBS*-related transgenic lines. *EBS:Flag* and pointed-muated *EBS:Flag* (*P41L* or *Y155A*), driven by a native *EBS* promoter, were introduced into *FRI ebs shl*. (G) Phenotypes of *SHL*-related transgenic lines. *HA:SHL* and pointed-mutated *HA:SHL* (*W63L/Y65A* or *F141A/Y148A*), driven by a native *SHL* promoter, were introduced into *FRI ebs shl*. Note that *HA:SHL* is fully functional. (D-G) Scale bars represent 1 cm.

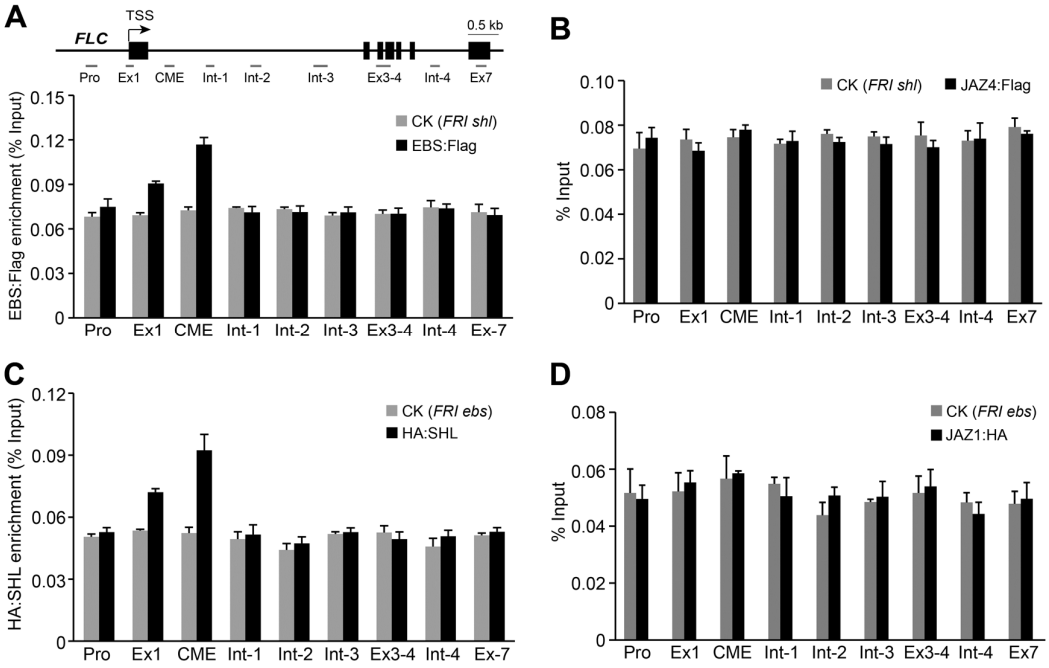

Figure S2. ChIP-qPCR analysis of EBS and SHL enrichment at *FLC* in the indicated seedlings (prior to cold exposure), related to Figure 1. (A) EBS:Flag enrichments across the *FLC* locus. Levels of the *FLC* fragments immunoprecipitated by anti-Flag were quantified by qPCR and normalized to input DNA. *FRI shl* serves as a background control (CK). On top is a schematic drawing of the *FLC* locus, and grey bars for the regions examined by ChIP. (B) A negative control for anti-Flag ChIP at the *FLC* locus. The transgenic line of *JAZ4:Flag* has been described in *ref S2*. The levels of background *FLC* fragments were normalized to input DNA. Note that the levels of background *FLC* fragments in CK (*FRI shl*) and the negative control of *JAZ4:Flag* are low, and very similar in all of the examined regions. (C) HA:SHL enrichments across *FLC*. Levels of the immunoprecipitated *FLC* fragments were normalized to input DNA. *FRI ebs* serves as a background control. (D) A negative control for anti-HA ChIP at *FLC*. *JAZ1:HA* has been described in *ref S2*. The levels of background *FLC* fragments were normalized to input DNA. (A-D) Error bars denote s.d. of three biological replicates.

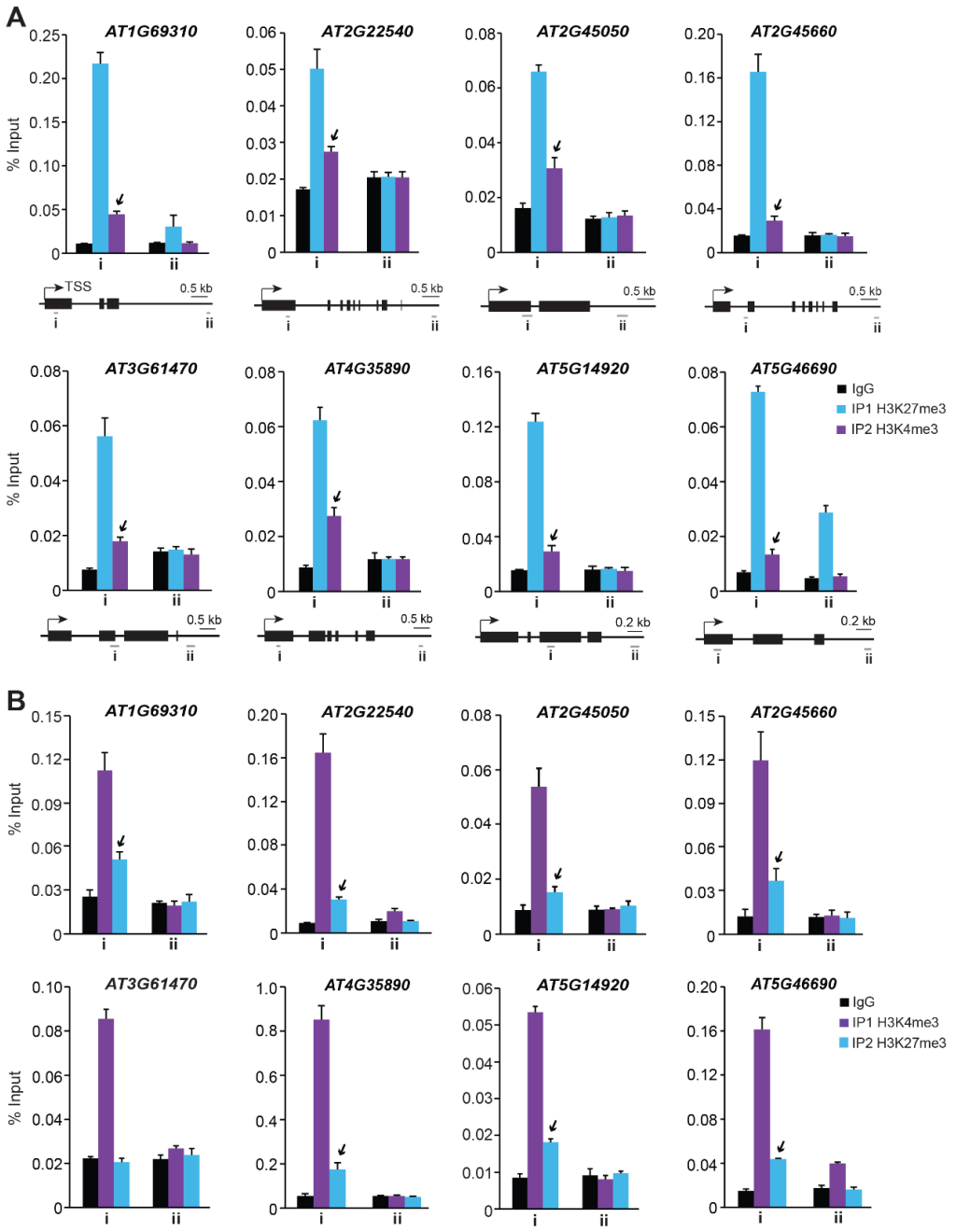

Figure S3. Validation of bivalency at eight selected H3K4me3-H3K27me3 loci by sequential ChIP assays, related to Figure 2. (A, B) Sequential K27-K4 reChIP (A) or K4-K27 reChIP (B). These eight loci are selected from a list of overlapped loci extracted from the ChIP-seq data of H3K4me3 and H3K27me3 (NCBI GEO accession nos.: GSE185121 and GSE185120). At bottom of each bar graph is a schematic drawing of the examined locus: arrow for the transcription start site, black boxes for exons, and grey bars for the regions examined by reChIP-qPCR. Levels of the immunoprecipitated DNA fragments were quantified by qPCR and normalized to input DNA; error bars denote s.d. of three biologically independent replicates. IgG, reChIP (the second ChIP) with rabbit IgG as negative control. Arrows on bar graphs indicate H3K4me3 (A) or H3K27me3 (B) enrichments.

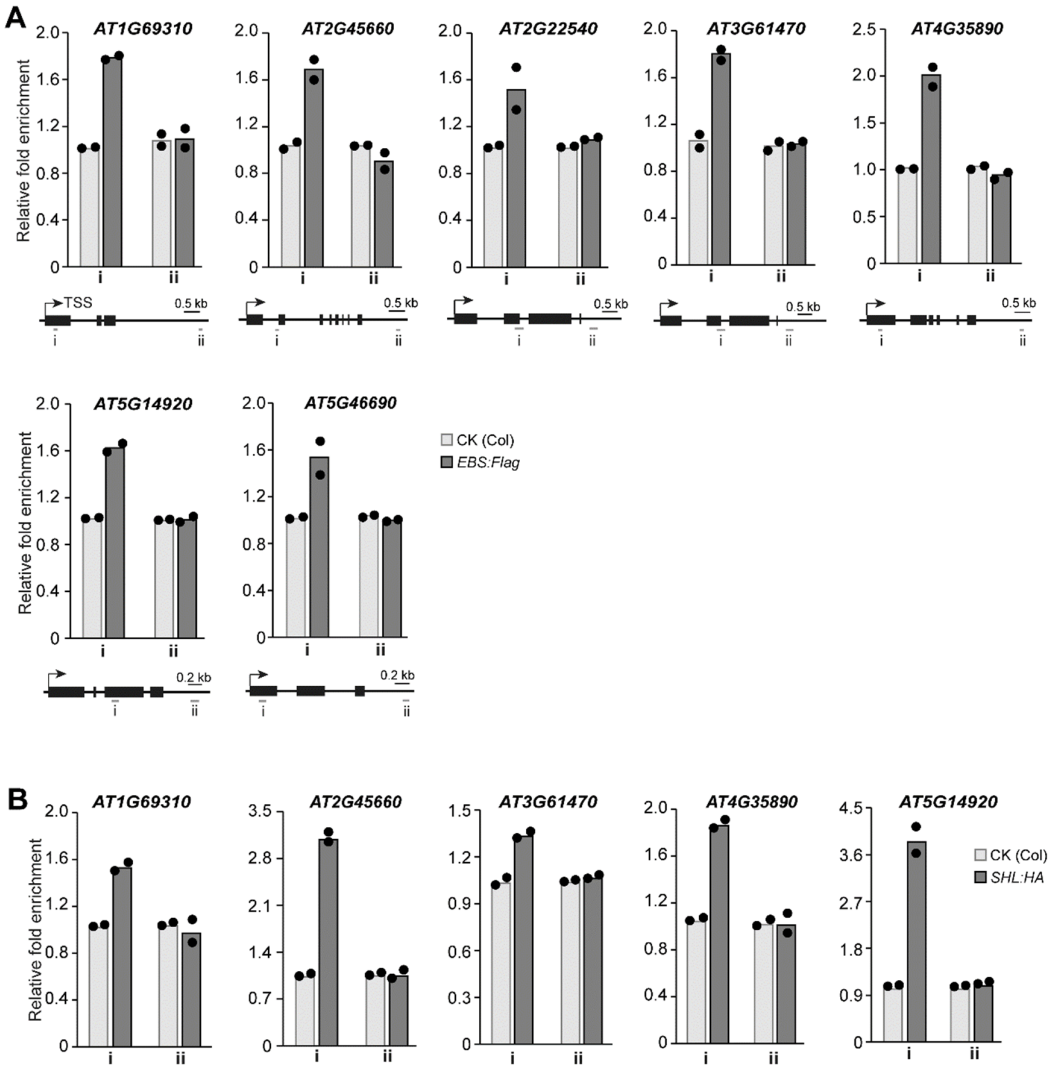

Figure S4. EBS and/or SHL bind to bivalent regions, related to Figure 2. (A, B) ChIP-qPCR analysis of EBS:Flag (A) and SHL:HA (B) binding to bivalent regions at the indicated bivalent loci. At bottom of each bar graph is a schematic drawing of the examined locus. EBS:Flag and SHL:HA are in *ebs shl*. Levels of the DNA fragments immunoprecipitated by anti-Flag or anti-HA were normalized first to the internal control *TUB2*; relative enrichments of EBS:Flag or SHL:HA over a background control (Col) are shown in dot plots (two biological replicates). Notably, it has been previously shown that part of the *AT2G45660* locus is bound by SHL.[S3]

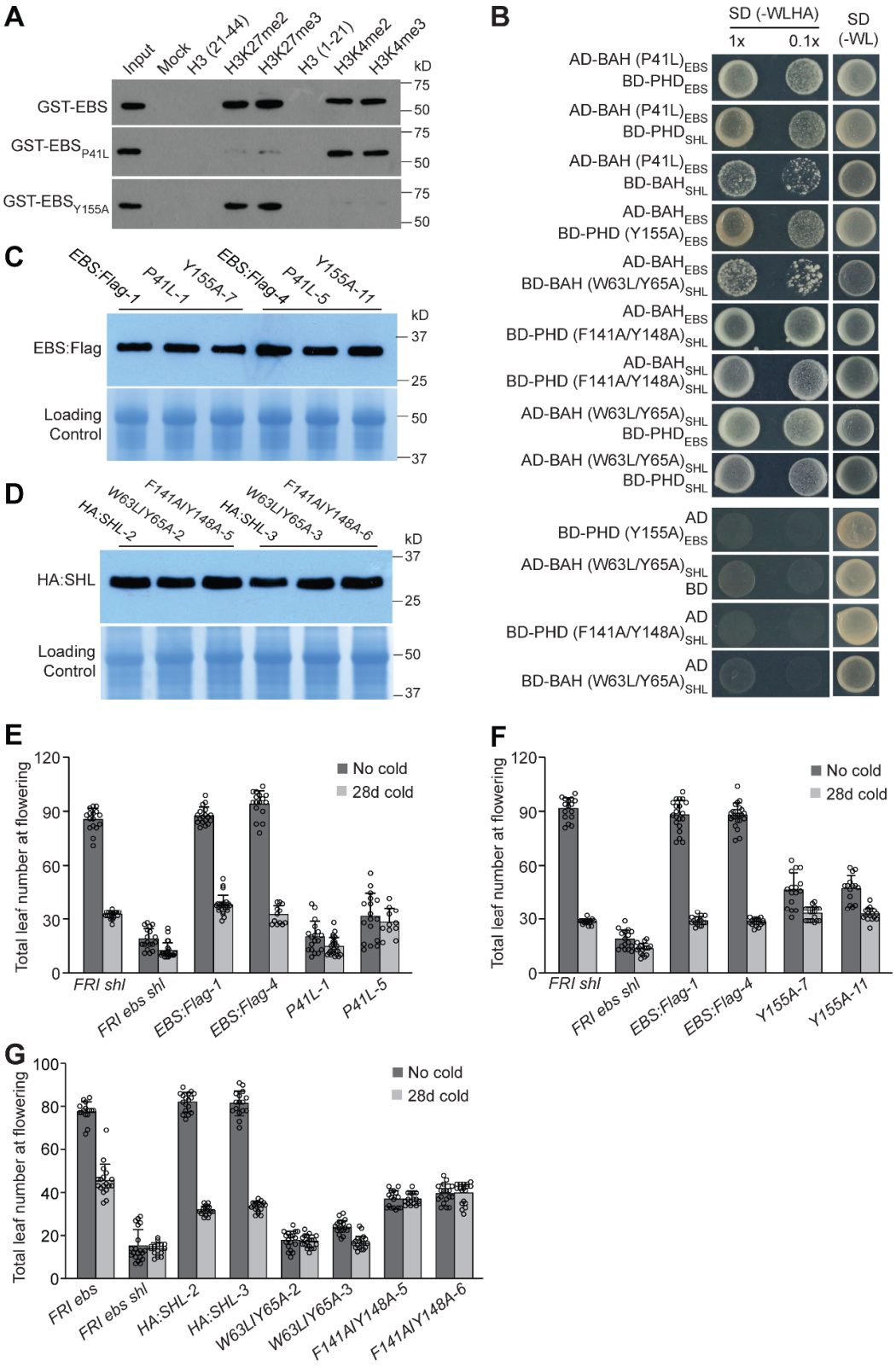

Figure S5. Analysis of point-mutated BAH and PHD domains in EBS and SHL. Related to Figure 3. (A) Pulldown of GST-EBS, GST-EBS$_{P41L}$ and GST-EBS$_{Y155A}$ by K4- or K27-modified H3 peptides. Western blotting assays were conducted with anti-

GST. (B) Point mutations in the BAH and PHD domains of EBS and SHL have no effect on BAH-BAH/PHD interactions in yeast cells. Mutated BAH or PHD domains were fused with the GAL4-AD or BD domain, as indicated. Yeast cells were spread on the stringent SD (-WLHA), and colonies on SD (-WL) served as growth control. (C, D) Western blotting analysis of EBS:Flag (C) or HA:SHL (D) abundance in the indicated seedlings. Duplicate protein gels stained with Coomassie Blue serve as loading controls. (E, F) Flowering-time measurements of transgenic plants expressing mutated BAH_{EBS} (E) or PHD_{EBS} (F) with and without 28-d cold treatment (vernalization). Small circles for individual data points, and error bars for s.d. (G) Flowering-time measurements of the indicated lines with and without 28-d cold treatment. Small circles for individual data points, and error bars for s.d.

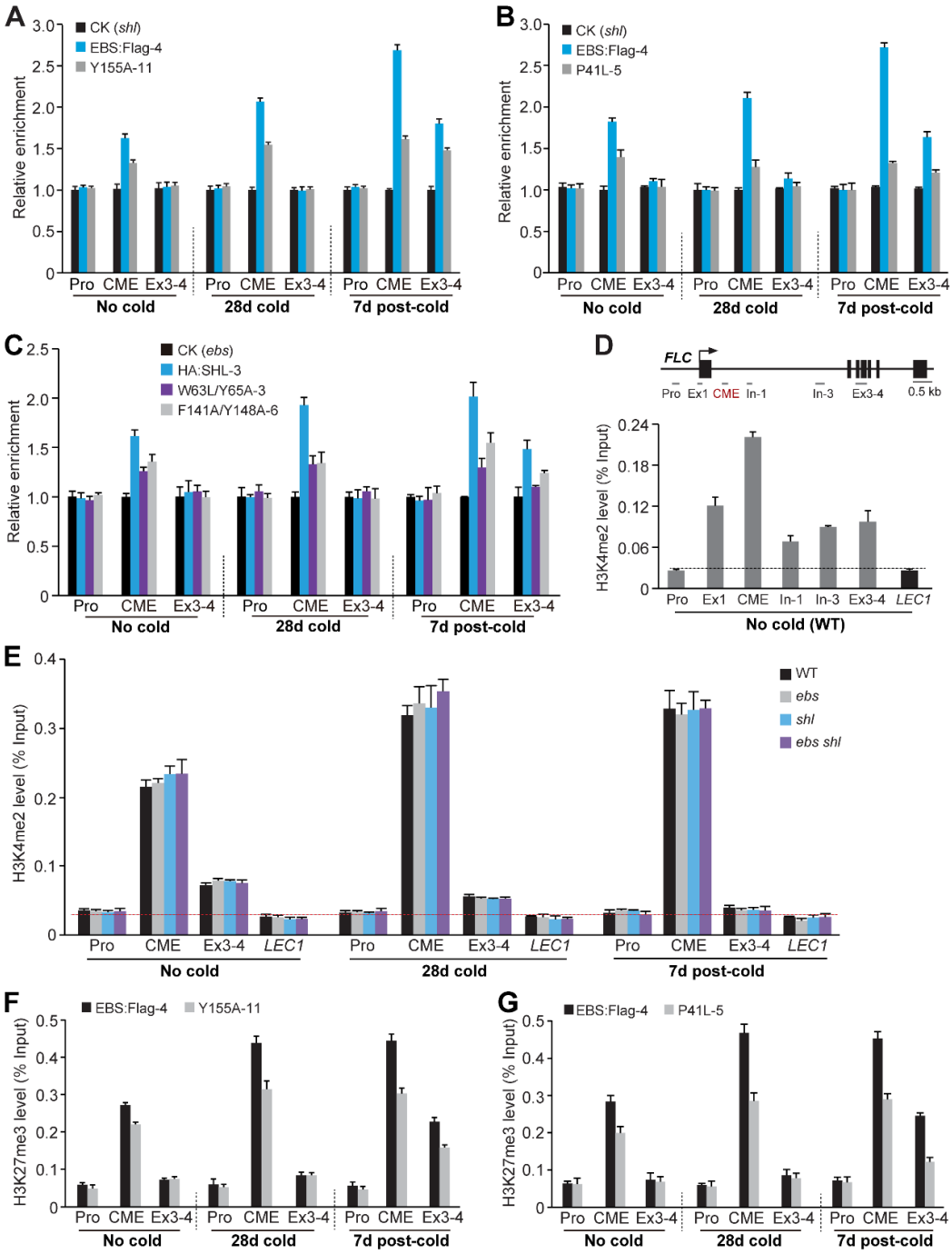

Figure S6. Functional analysis of the BAH and PHD domains in EBS and SHL and measurement of H3K4me2 on *FLC* chromatin, related to Figures 3 and 5. (A, B) ChIP-qPCR analysis of EBS$_{Y155A}$ (A) and EBS$_{P41L}$ (B) enrichments at *FLC* after 28-d cold exposure. Relative enrichment of wild-type or point-mutated EBS:Flag over a background control (*FRI shl*) is calculated, as described in the Figure 3 legends. (C) ChIP-qPCR analysis of SHL, SHL$_{W63L/Y65A}$ and SHL$_{F141A/Y148A}$ enrichments at *FLC* after 28-d cold. (D-E) ChIP analysis of H3K4me2 on *FLC* chromatin. DNA fragments were immunoprecipitated by anti-H3K4me2 from the seedlings of WT, *ebs*, *shl* and *ebs shl*, and subsequently, the indicated regions were quantified by qPCR. Notably, the WT

samples of 'no cold' were quantified in both (D) and (E). The vegetative phase-silenced *LEAFY COTYLEDON 1* (*LEC1*) locus,[S4] serves as a background control (lack of H3K4me2). Data are mean ± s.d. of three biological replicates. (F-G) ChIP analysis of H3K27me3 at *FLC* in the lines of H3K4me3-binding defective EBS:Flag (Y155A) (F) or H3K27me3-binding defective EBS:Flag (P41L) (G) in response to 28-d cold exposure. A transgenic line expressing wild-type EBS:Flag serves as control. Error bars in (A-C) and (F-G) denote s.d. of three quantifications (technical replicates).

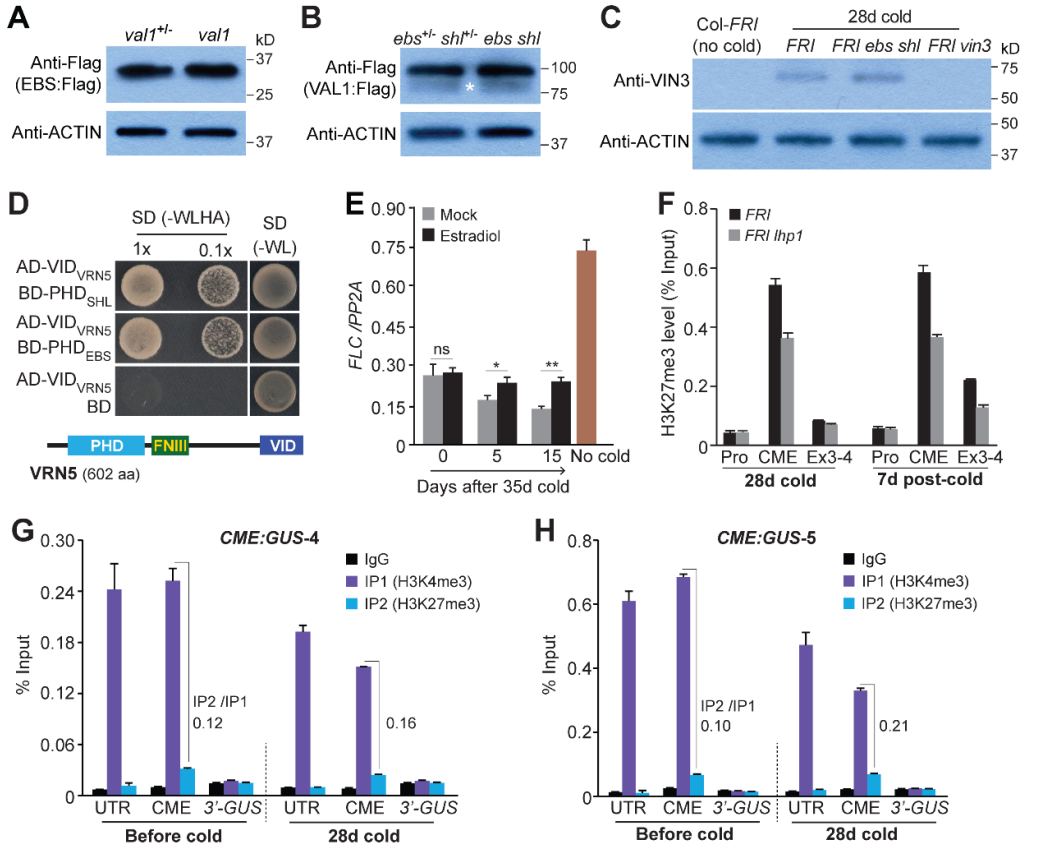

Figure S7. Analysis of cold-induced Polycomb repression of *FLC* by CME and the chromatin-associated factors, related to Figures 4 and 6. (A, B) Levels of EBS:Flag (A) and VAL1:Flag (B) in the indicated seedlings, analyzed by western blotting. In (A), an *EBS:Flag FRI val1* line was crossed to *FRI val1* and WT to obtain the F_1 seedlings of *val1*$^{+/-}$ (*FRI EBS:Flag*) and *val1* (*FRI EBS:Flag*). In (B), a *VAL1:Flag FRI ebs shl* line was crossed to *FRI ebs shl* and WT to obtain the F_1 seedlings of *ebs*$^{+/-}$ *shl*$^{+/-}$ (*VAL1:Flag FRI*) and *ebs shl* (*VAL1:Flag FRI*). Levels of ACTIN serve as loading control. Star in (B) denotes a degradation product of VAL1. (C) Levels of the cold-induced VIN3 protein in the WT (Col-*FRI*), *ebs shl* and *vin3* seedlings after 28-d cold exposure, analyzed by western blotting using a rabbit polyclonal anti-VIN3. (D) The VID domain of VRN5 (VID_{VRN5}, aa 502 to 602) interacted with the PHD domains from EBS and SHL in yeast cells. Cells were grown on the highly stringent media of SD (-WLHA). (E) Re-activation of *FLC* expression upon specific *VAL1* knockdown on return to the warm. *FLC* levels were normalized to *PP2A*. 'No cold', non-vernalized plants at about the same developmental stage as the plants grown for 15 d after cold. Error bars indicate s.d. of three biological repeats. Data were evaluated by two-tailed *t* tests; ns for not significant; * $p<0.05$; ** $p<0.01$. (F) ChIP analysis of H3K27me3 at *FLC* in the seedlings of WT and *FRI lhp1* in response to 28-d cold exposure. (G, H) Sequential H3K4me3-H3K27me3 ChIP assays on *CME:GUS* chromatin in *CME:GUS*-4 (G) and -5 (H) seedlings at the indicated conditions. Levels of *CME:GUS* fragments were normalized to input DNA. IgG, reChIP with IgG as negative control. Error bars denote s.d. of three quantifications. Ratios of the level of H3K27me3 recovered from IP2 (reChIP) to H3K4me3 from IP1 are denoted.

Table S1. Oligos used in this study, related to STAR Methods

Experiment	Amplified region	Sequence (5'-3')
Plasmid Construction	*gEBS.2* (F)	AATGGATCCTAATGGATTCACTGTAGATGATGGA
	gEBS.2 (R)	TCCCTCGAGCCTTTTTCTGCGCTTCGTT
	EBS.2-P41L (F)	GTGTGTTGATGCGCCTATCAGATGCTGGTAAAC
	EBS.2-P41L (R)	GTTTACCAGCATCTGATAGGCGCATCAACACAC
	EBS.2-Y155A (F)	CAAATGTGAAATGCCTGCCAATCCAGACGATCTC
	EBS.2-Y155A (R)	GAGATCGTCTGGATTGGCAGGCATTTCACATTTG
	gSHL (F)	AGTGGATCCGGAGATGTGTGTGATATTTCTATATT
	gSHL (R)	GAACTCGAGAAGGAGAGAGTTAACCAATGATGTA
	SHL-W63L/Y65A(F)	GAAAGTTCGTGTGAGGCTGTATGCGCGCCCTGAGGAA TCTATC
	SHL-W63L/Y65A(R)	GATAGATTCCTCAGGGCGCGCATACAGCCTCACACGA ACTTTC
	SHL-F141A/ Y148A) (F)	CTGTTTGCAGGGCCTGCAAGTGTGAGATGCCGGCAAA CCCAGATGACTTG
	SHL-F141A/ Y148A) (R)	CAAGTCATCTGGGTTTGCCGGCATCTCACACTTGCAG GCCCTGCAAACAG
RT-qPCR	*PP2A* (F)	TATCGGATGACGATTCTTCGTGCAG
	PP2A (R)	GCTTGGTCGACTATCGGAATGAGAG
	VAL1 (F)	ACTCTTAGTGCCAGTGATGC
	VAL1 (R)	ACTCCCTACCCCTCACATC
	FLC (F)	CCGAACTCATGTTGAAGCTTGTTGAG
	FLC (R)	CGGAGATTTGTCCAGCAGGTG
	FT (F)	GACCTCAGGAACTTCTATACTTTGGTTATG
	FT (R)	CTGTTTGCCTGCCAAGCTG
	TUB2 (F)	GCCTTGTACGATATTTGCTTCAGGAC
	TUB2 (R)	CGGAGGTCAGAGTTGAGTTGAC
Unspliced mRNA RT-qPCR	*PP2A* (F)	ACTTGTTCAGGTTCTAGAGATGATT
	PP2A (R)	CATTTGAATATATGGACGTT
	CME:GUS (F)	TGGCGCCTGGTTAAGTAAAG
	CME:GUS (R)	GCATTAGAACAATAATTTATG
ChIP-qPCR	*FLC* P0 (F)	TGGATTGATGTGGGGCACTATTAAGT
	FLC P0 (R)	GGTTGTTCCCTCCAAACCAATTTGAG
	FLC Pro (F)	CAAGCTGATACAAGCATTTCACCAA
	FLC Pro (R)	TGTCCACACATATGGCAATAGCTCAA
	FLC Ex1 (F)	CCGACGAAGAAAAAGTAGATAGGCAC
	FLC Ex1 (R)	CCTAATTTGATCCTCAGGTTTGGG

ChIP-qPCR	*FLC* CME (F)	TTCTGCGACCATGATAGATACAT
	FLC CME (R)	GGAAATAATGAAATCCATGCAGA
	FLC In-1 (F)	GTTCTCTTGGATTTGTATATGCACGTC
	FLC In-1 (R)	CCAATTCATCTTTTAGTCATAGTTTCCC
	FLC In-2 (F)	GCCTTTTAGAACGTGGAACCC
	FLC In-2 (R)	AGAAGGAAGCGACTAAGACAGA
	FLC In-3 (F)	GAAGCAGTCTTCCACTATTTGCTATTGT
	FLC In-3 (R)	ACGCAGCCCCAATCTTAAATGC
	FLC Ex3-4 (F)	TGGGCAGGATCATCAGTCAA
	FLC Ex3-4 (R)	AGGGCAGTCTCAAGGTGTTC
	FLC In-4 (F)	CGGCTGGTTAGAGTTAAGGGAAATC
	FLC In-4 (R)	AAAACGAAGAAGAAGAACCAAAACC
	FLC Ex7 (F)	GAGATGGAGATGTCACCTGCTGG
	FLC Ex7 (R)	CAAACGCTCGCCCTTATCAGC
	CME:GUS 5'UTR (F)	CCATCCATTCACGGCCAAG
	CME:GUS 5'UTR (R)	CTGGAGCCGCTAGAGAAGAA
	CME:GUS CME (F)	TCTTGATGTTCGTTTCGTGTTT
	CME:GUS CME (R)	TTACTTAACCAGGCGCCAGG
	CME:GUS 3'*GUS* (F)	CGTCGGTGAACAGGTATGGA
	CME:GUS 3'*GUS* (R)	CGAAGTTCATGCCAGTCCAG
	STM (F)	GCCCATCATGACATCACATC
	STM (R)	GGGAACTACTTTGTTGGTGGTG
	LEC1 (F)	AGTCTACTCAACGGGGTCCATA
	LEC1 (R)	TGTGCTGGTCCAAGTTCAATTC
	TUB2 (F)	ATCCGTGAAGAGTACCCAGAT
	TUB2 (R)	AAGAACCATGCACTCATCAGC
Sequential ChIP-qPCR	*AT2G45660*-i (F)	TTGCACCATTGATCTACCGTTTTCT
	AT2G45660-i (R)	GAGTTTTGCCCCTCACCATATCTTC
	AT2G45660-ii (F)	CCAAGGTCAACTACGTGGCATTTTA
	AT2G45660-ii (R)	CAAAGGAGGATTCAGCTCAACTACG
	AT1G69310-i (F)	TCTGACTTCTTCGACCGAGACACTT
	AT1G69310-I (R)	TGACTCCGGTGGTTTGTGTTAAATC
	AT1G69310-ii (F)	TATTTTCCATGGGCTTGGGAGTAAC
	AT1G69310-ii (R)	TGCCTCAGCTTTTCAGCTAAACATA
	AT5G14920-i (F)	CCCACGCTGCCAACTACTCCTATTA
	AT5G14920-i (R)	GAGTTGAAACCGGAGGTTTTACTGG
	AT5G14920-ii (F)	CAGTTGGGTCAAATGCTCTAATTGC
	AT5G14920-ii(R)	GCAAGACTTTCCCAAATGATCTTCA

Sequential ChIP-qPCR	*AT2G45050*-i (F)	TCTTCTTCTTTCCCTCCTCCTCAAA
	AT2G45050-i (R)	GAGGGAGAGAGATTATACGGGAACG
	AT2G45050-ii (F)	GAAGCATGAAATCAGAAAAAGCTTCA
	AT2G45050-ii (R)	TTTGATCGAAACGTGAAGTCGAAAT
	AT2G22540-i (F)	ATCCATCAAAATCAATCCCGTTCTC
	AT2G22540-i (R)	TCTGAATCTTTTCTCTCGCCATCAC
	AT2G22540-ii (F)	GTTTAAACCGTCACAAAGGGGAAAA
	AT2G22540-ii (R)	TGGATAAAGGAATGTGAAAATGTCG
	AT4G35890-i (F)	CCACTTCCAATAACCCTGCTTCTTC
	AT4g35890-i (R)	GAGAAGAAACCTGCCGAGAAGGAC
	AT4G35890-ii (F)	CGATCTAGTTATCCAAGGCCCTCTC
	AT4G35890-ii (R)	TTCTTGGGCCGTTTCTGATTATTTT
	AT3G61470-i (F)	ACTCCTCCAGAGTGGCTAGACGGTA
	AT3G61470-i (R)	TAAAAAGCATGCAAGGAGGAACAAA
	AT3G61470-ii (F)	TTGTGGTCGAATGCAAATTAAGGTT
	AT3G61470-ii (R)	TGGACTCTTTTATGCTCCGAATGAC
	AT5G46690-i (F)	TGAAACTCTTTCACCAACTCCATTCA
	AT5G46690-i (R)	GTGGTGGCGGTTCTTGATTAGATA
	AT5G46690-ii (F)	GACCTTTCTCCAGTGGCCCATATTA
	AT5G46690-ii (R)	AAGTGAAGTACTCTCGCCTCTGTTGC

SUPPLEMENTAL REFERENCES

S1. Lee, I., Michaels, S.D., Masshardt, A.S., and Amasino, R.M. (1994). The late-flowering phenotype of *FRIGIDA* and *luminidependens* is suppressed in the Landsberg *erecta* strain of *Arabidopsis*. Plant J. *6*, 903-909.

S2. Li, Z., Luo, X., Ou, Y., Jiao, H., Peng, L., Fu, X., Macho, A.P., Liu, R., and He, Y. (2021). JASMONATE-ZIM DOMAIN proteins engage Polycomb chromatin modifiers to modulate Jasmonate signaling in Arabidopsis. Mol. Plant *14*, 732-747.

S3. Qian, S., Lv, X., Scheid, R.N., Lu, L., Yang, Z., Chen, W., Liu, R., Boersma, M.D., Denu, J.M., Zhong, X., and Du, J. (2018). Dual recognition of H3K4me3 and H3K27me3 by a plant histone reader SHL. Nat Commun. *9*, 2425.

S4. Tao, Z., Shen, L., Gu, X., Wang, Y., Yu, H., and He, Y. (2017). Embryonic epigenetic reprogramming by a pioneer transcription factor in plants. Nature *551*, 124-128.